Dark Matter Halos

A. Klypin (UVa, NMSU)

- **Dark matter halos profiles:**
  - **DM only: NFW vs. Einasto**
  - **Profiles at small and large scales**
  - **Halo concentration: evolution with time**
  - **Cores and cusps**

Bridging the gap between halos and galaxies

Abundance of halos at different redshifts

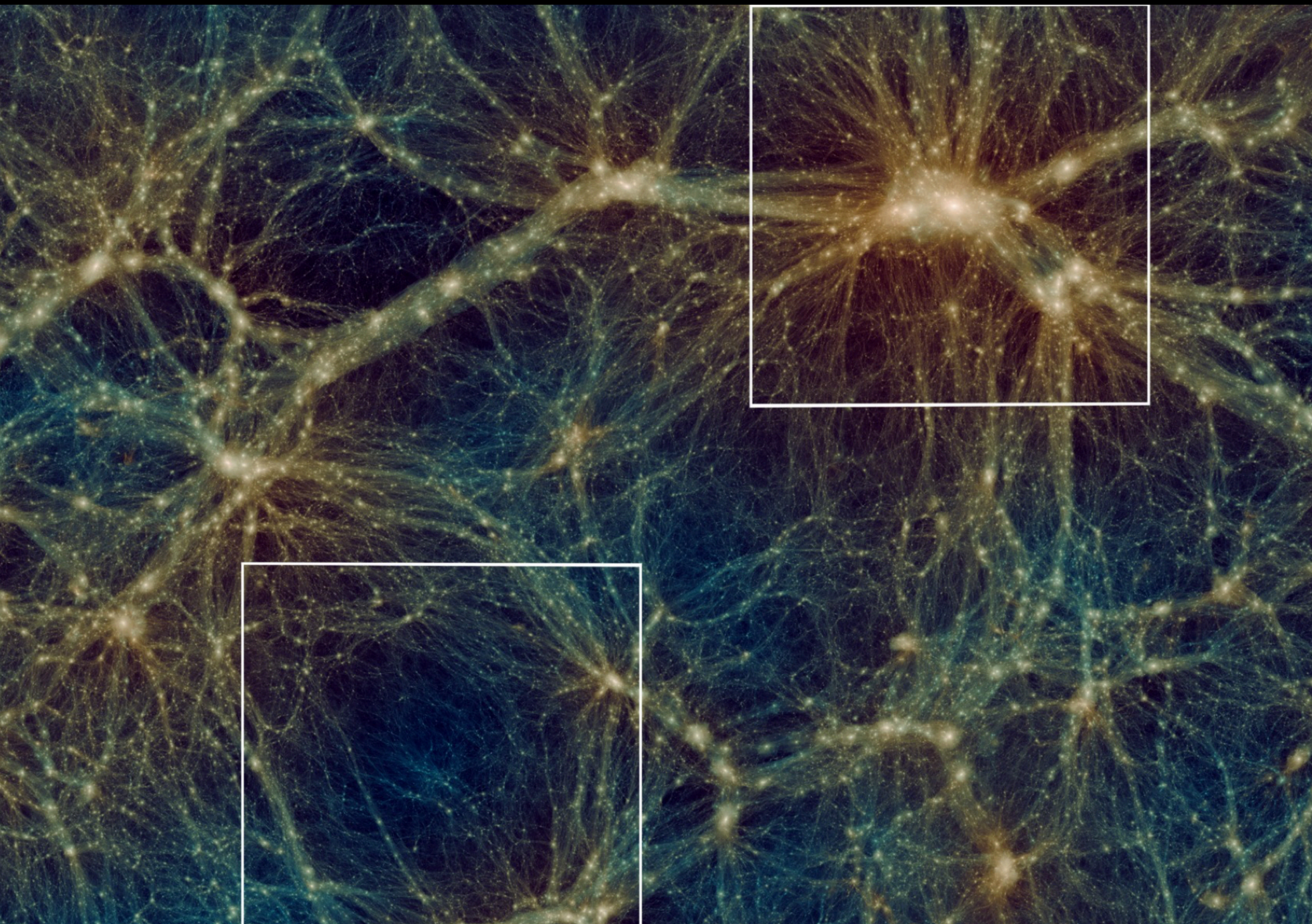

$$\rho(r) = \frac{\rho_0 r_s^3}{r(r + r_s)^2}\,, \quad M(r) = M_{\rm vir} \times \frac{f(x)}{f(C)}\,,$$

$$f(x) \equiv \ln(1 + x) - \frac{x}{1 + x}\,, \quad x \equiv \frac{r}{r_s}\,,$$

$$C \equiv \frac{r_{\rm vir}}{r_s}\,,$$

$$r_{\rm vir}(M_{\rm vir}) = 443\ h^{-1}\ {\rm kpc}\left(\frac{M_{\rm vir}/10^{11}\ h^{-1}\ M_\odot}{\Omega_0\,\delta_{\rm th}}\right)^{1/3}$$

$$M_{\rm vir} \equiv \frac{4\pi}{3}\,\rho_{\rm cr}\,\Omega_0\,\delta_{\rm th}\,r_{\rm vir}^3\,.$$

$$V_{\rm max}^2 = \frac{GM_{\rm vir}}{r_s} \times \frac{f(2)}{2f(C)}\,, \quad f(2) \approx 0.432\,,$$

$$M(r) = \frac{r_s\,V_{\rm max}^2}{G} \times \frac{2f(x)}{f(2)}\,, \quad \Omega^2(r) = \frac{V_{\rm max}^2}{r_s^2} \times \frac{2f(x)}{x^3 f(2)}\,,$$

$$V_{\rm esc}^2 = -2\phi(r) = 4V_{\rm max}^2 \times \frac{\ln(1 + x)}{xf(2)}\,,$$

NFW:

slope: -1 at small radii — divergent density

slope: -3 at large radii — divergent mass

Einasto:

$$\rho_{\rm Ein}(r) = \rho_0 \exp\left(-\frac{2}{\alpha}\left[x^\alpha - 1\right]\right), \quad x \equiv \frac{r}{r_{-2}}$$

the radius r_{-2} is the characteristic radius of the halo where the logarithmic slope of the density profile d log(ϱ)/d log(R) is equal to -2.

$$f_E(x,\alpha) = e^{\frac{2}{\alpha}} \int_0^x x^2 e^{-\frac{2}{\alpha}x^\alpha} dx,$$

$$x \equiv \frac{r}{r_{-2}}, \quad C = \frac{R_{\rm vir}}{r_{-2}}.$$

Densities and velocities at large distances

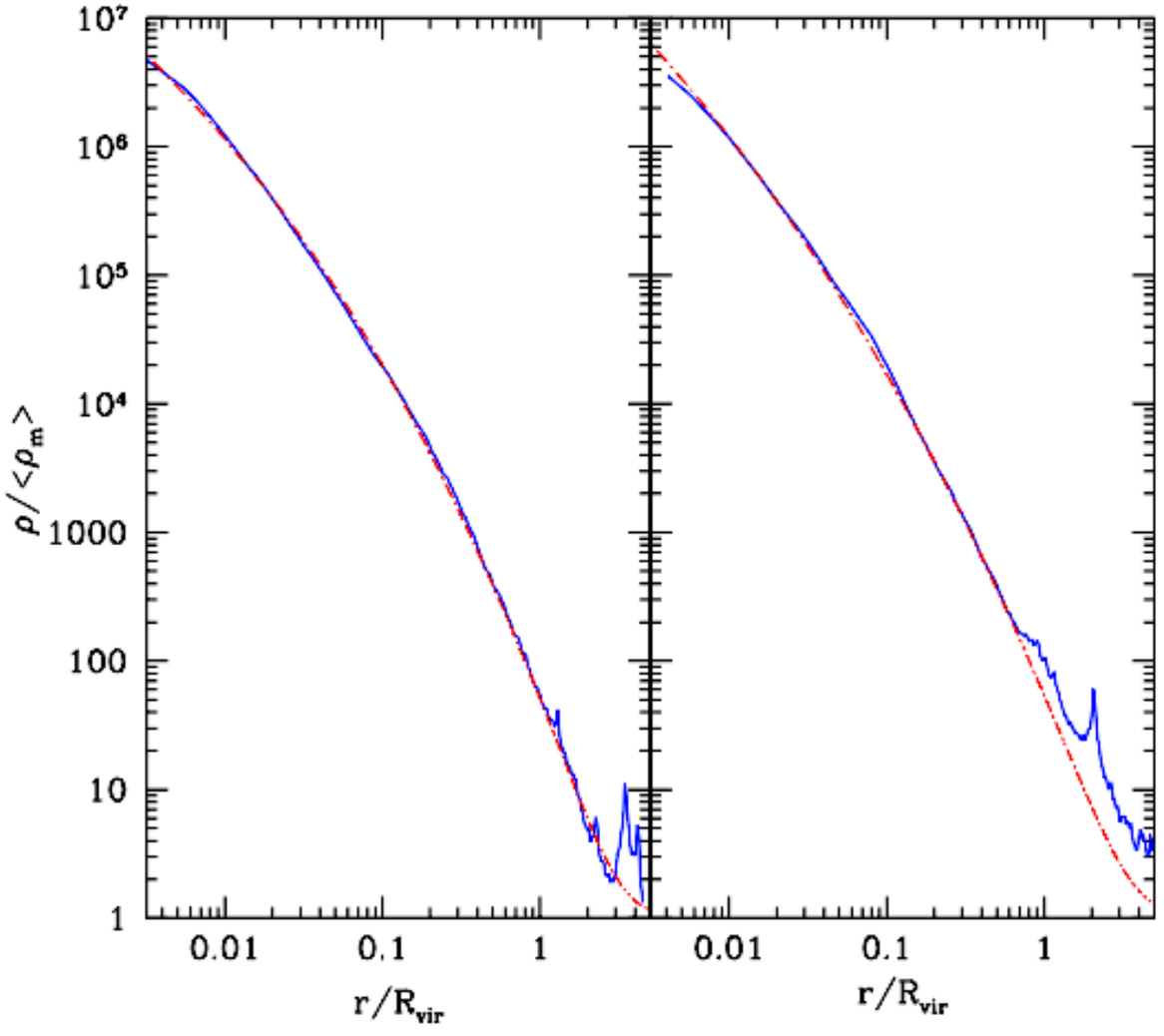

Fig. 1.— Dark matter density profiles of two dark matter halos (full curves) in the simulation Box20. The halos have virial masses of $1.4 \times 10^{12} h^{-1} M_\odot$ (left panel) and $2.6 \times 10^{11} h^{-1} M_\odot$ (right panel). The larger halo has a neighbour at 3.5 R_{vir} which is the halo on the right panel. This smaller halo is responsible for the spike at large radii in the density profile. In turn, the halo on the right panel has its own smaller neigbour at $2R_{vir}$ observed as a spike and an extended bump in the density profile. The dashed curves show the 3D Sersic profiles. The halo density profiles extend well beyond the formal virial radius with the Sérsic profile providing remarkably good fits. **Einasto**

Density profiles of halos with mass $M_{200} \approx 1.2 \times 10^{14} h^{-1} M_\odot$ at z = 1.5 (full curves). Dot-dashed curves show Einasto fits, which have the same virial mass as halos in the simulation. The NFW profiles (dashed curves) do not provide good fits to the profiles and significantly depend on what part of the density profile is chosen for fits.

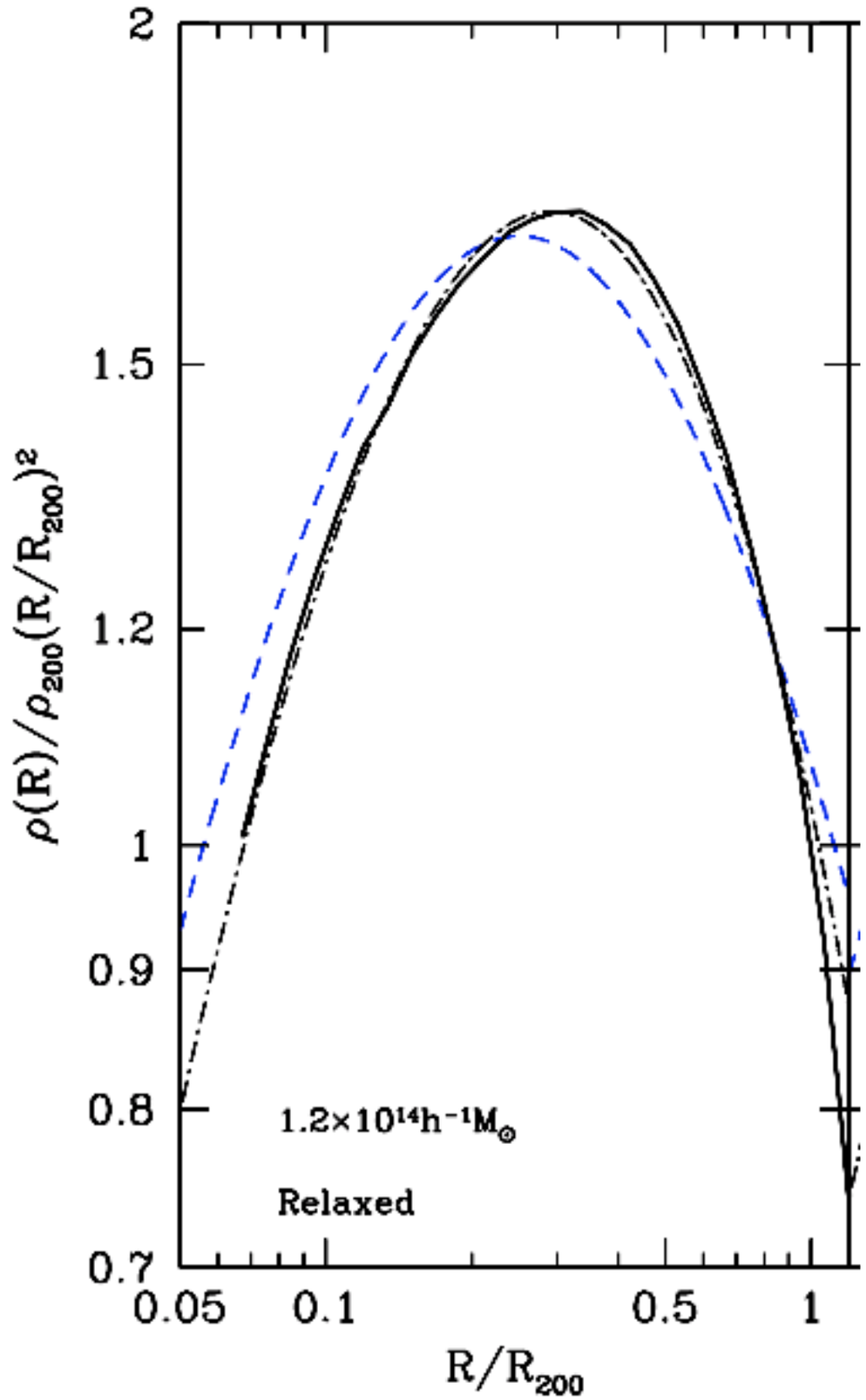

Dark matter profiles

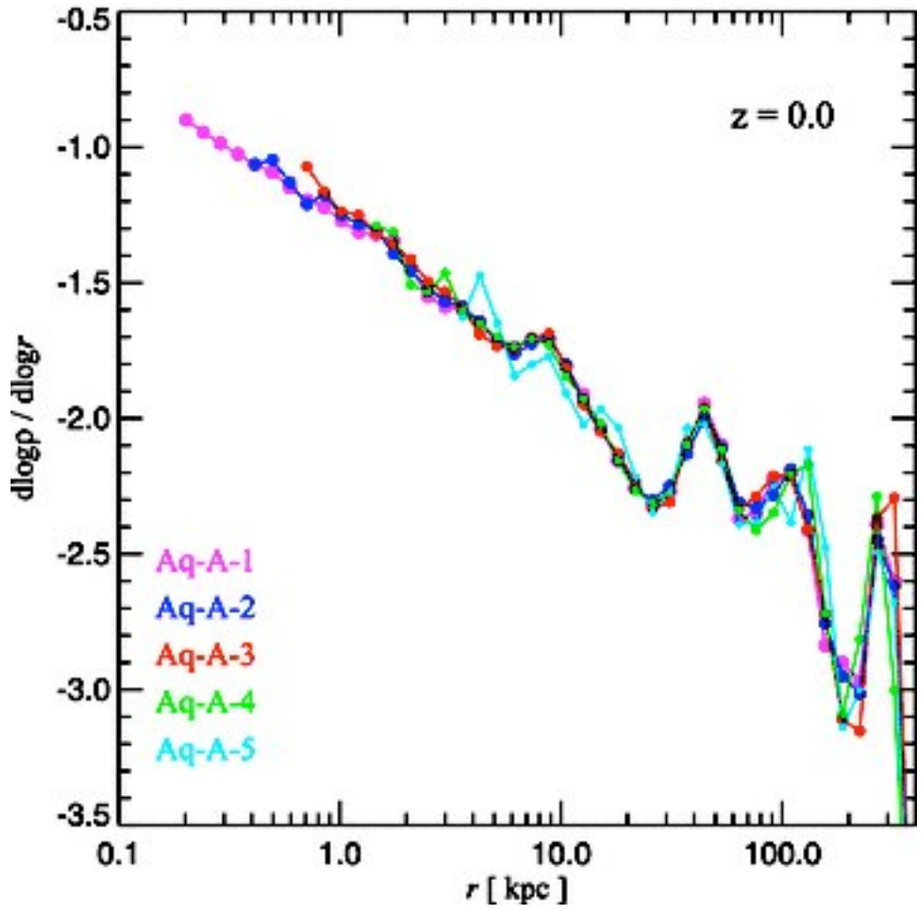

Aquarius simulation. Springel et al 2008. WMAP-1

Central slope is very close to -1

For normal galaxies it does not matter: baryons dominate in those regions and affect DM

Stadel etal 2009

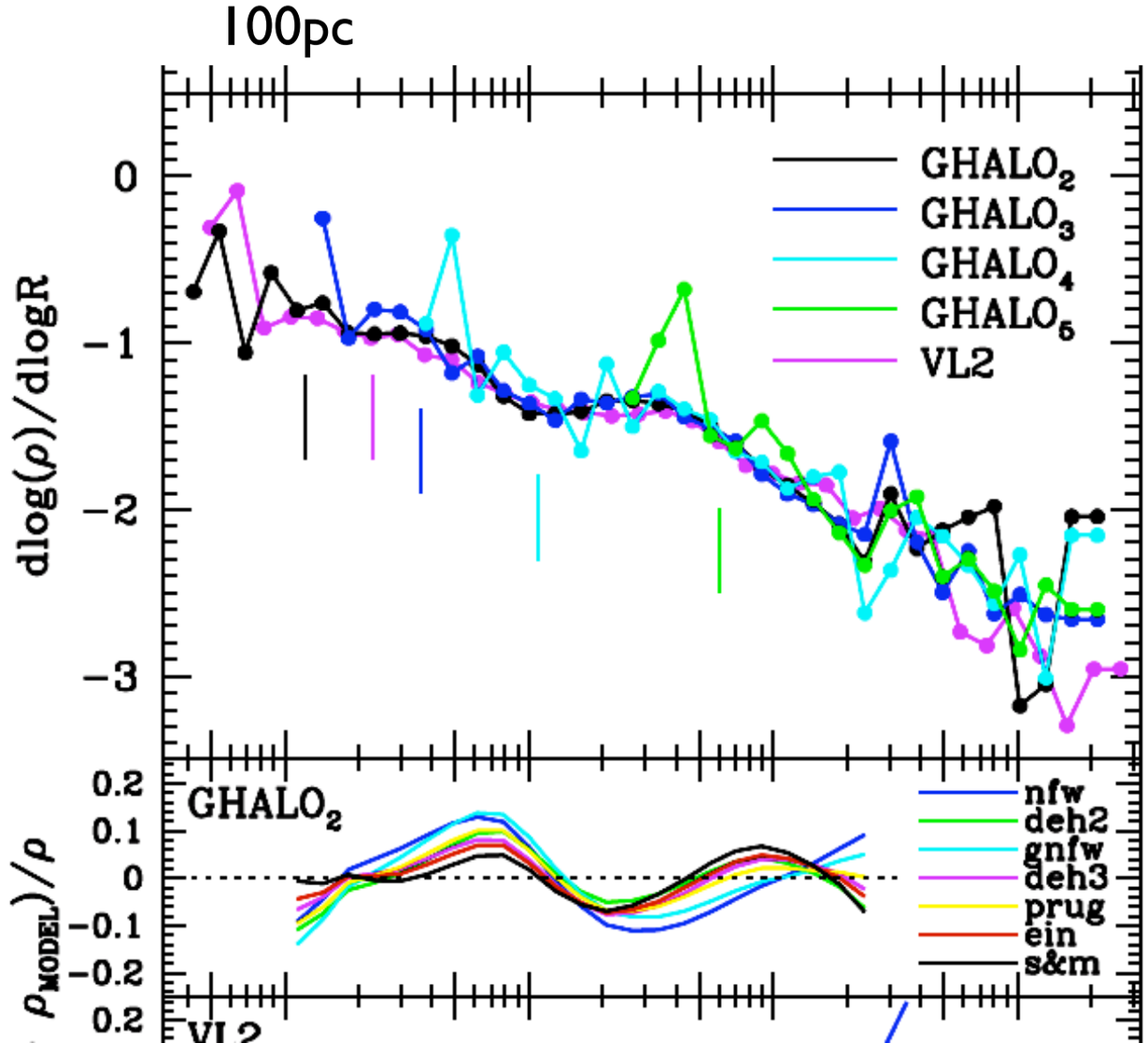

M=5x10^{12}

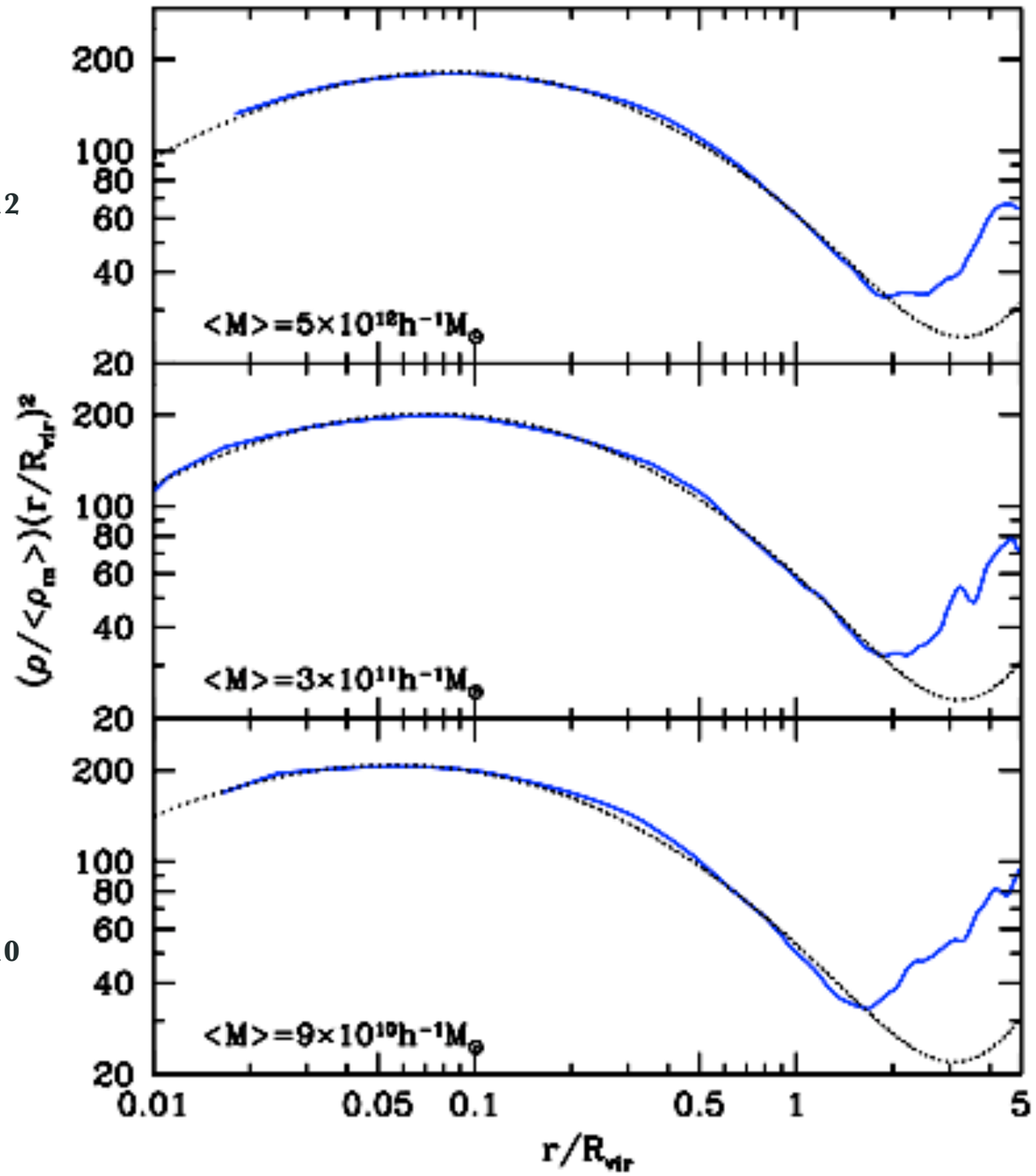

M=9x10^{10}

Fig. 3.— Average density profiles for halos with different virial masses. The 3D Sérsic profile provides very good fit with few percent errors within $2R_{vir}$. Even at $3R_{vir}$ the error is less than 20-30 percent. The density profiles are well above the average density of the Universe throughout all the radii.

3d Sersic = Einasto

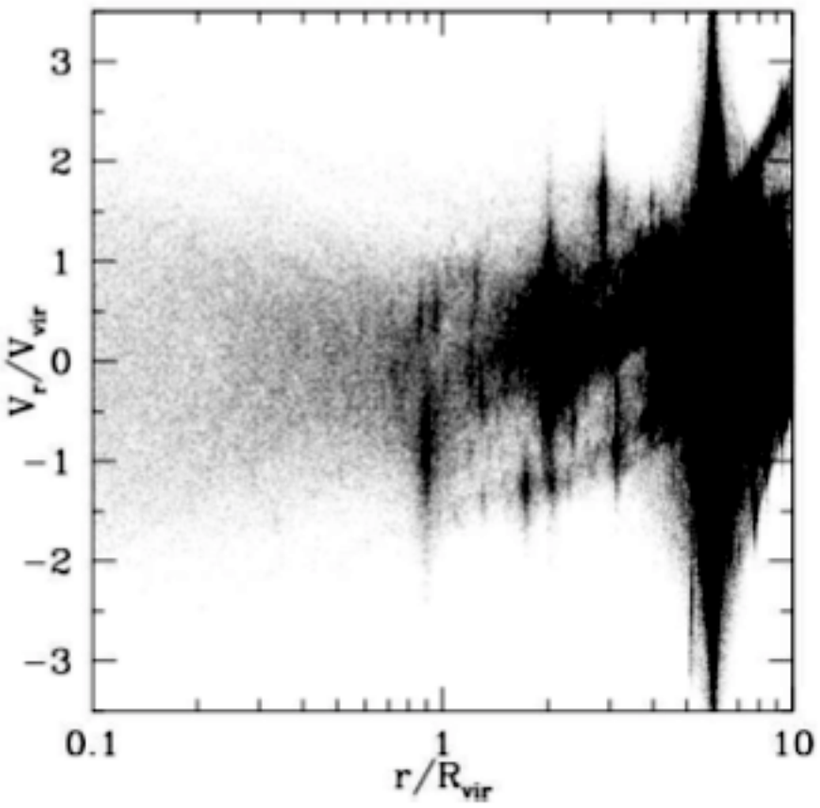

Phase-space diagram for the particles in dark matter halos

Mvir =3 10^{11}Msun

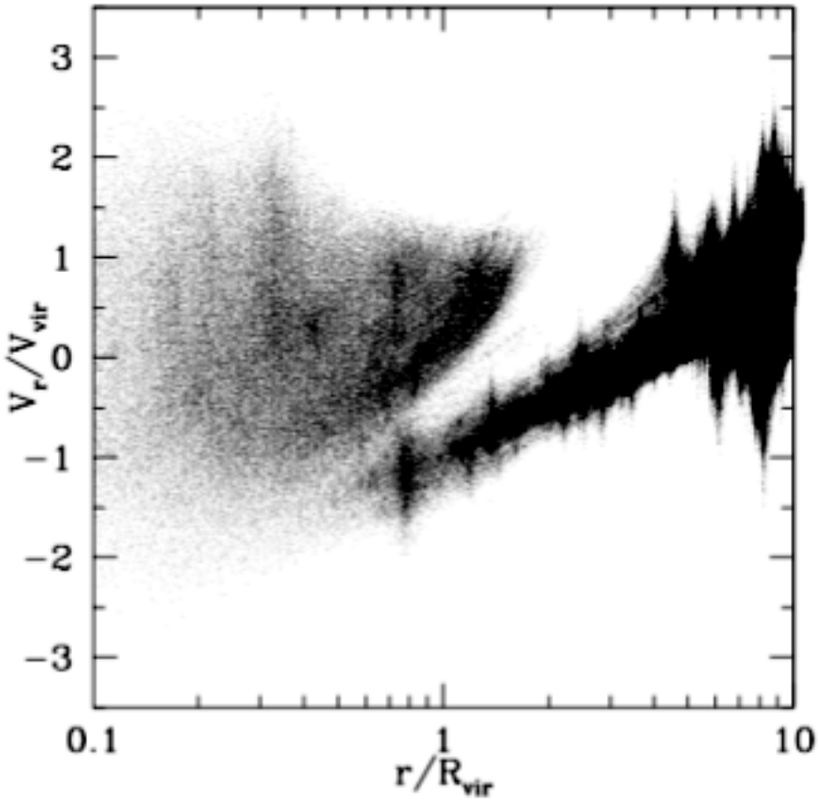

Mvir =1.5 10^{15}Msun

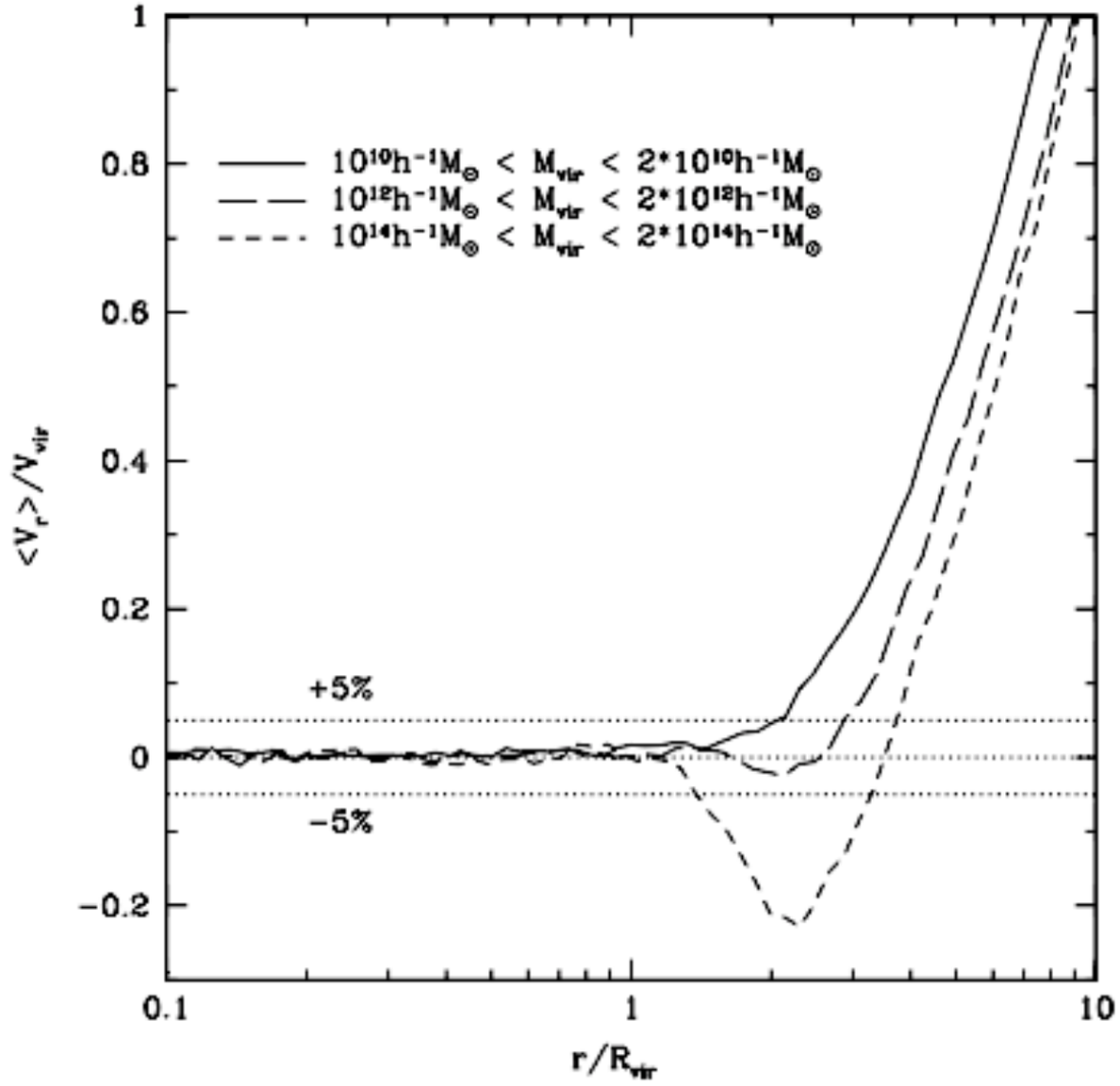

Figure 4. Mean radial velocity for three different mass bins. The profiles were obtained by averaging over hundreds of distinct haloes on each mass bin. In dotted line is shown the selected threshold delimiting the static region (5 per cent of the virial velocity). Cluster-size haloes display a region with strong infall (dashed line). On the contrary, low-mass haloes (solid line) and galactic haloes (long-dashed line) do not show infall at all but a small outflow preceding the Hubble flow.

Velocity anisotropy

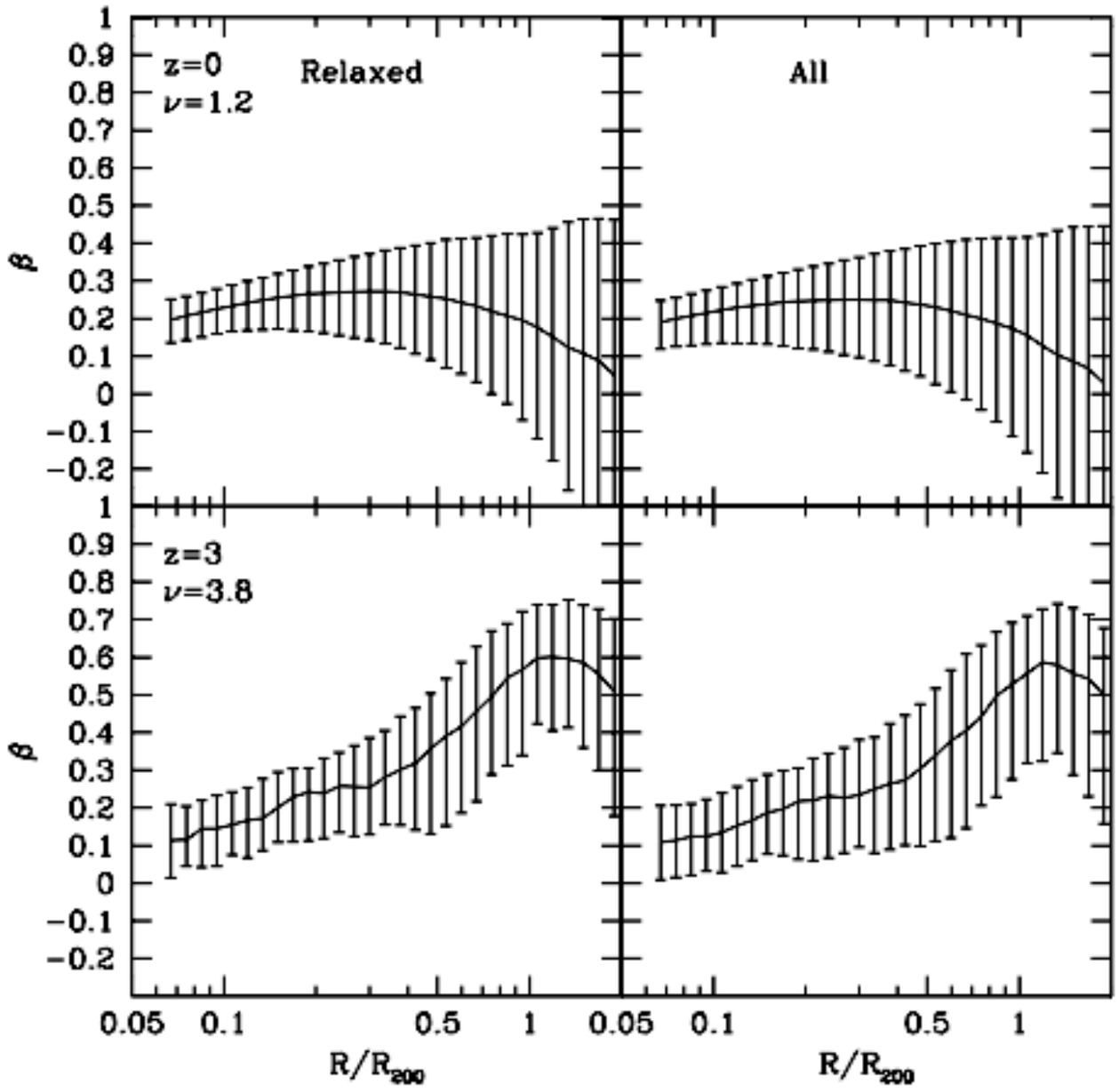

δ_{cr}/σ

M=10^{13}Msun

$$\beta = 1 - \frac{\sigma_t^2}{\sigma_r^2},$$

where σ_r^2 is the radial velocity dispersion and σ_t^2 is the tangential velocity dispersion.

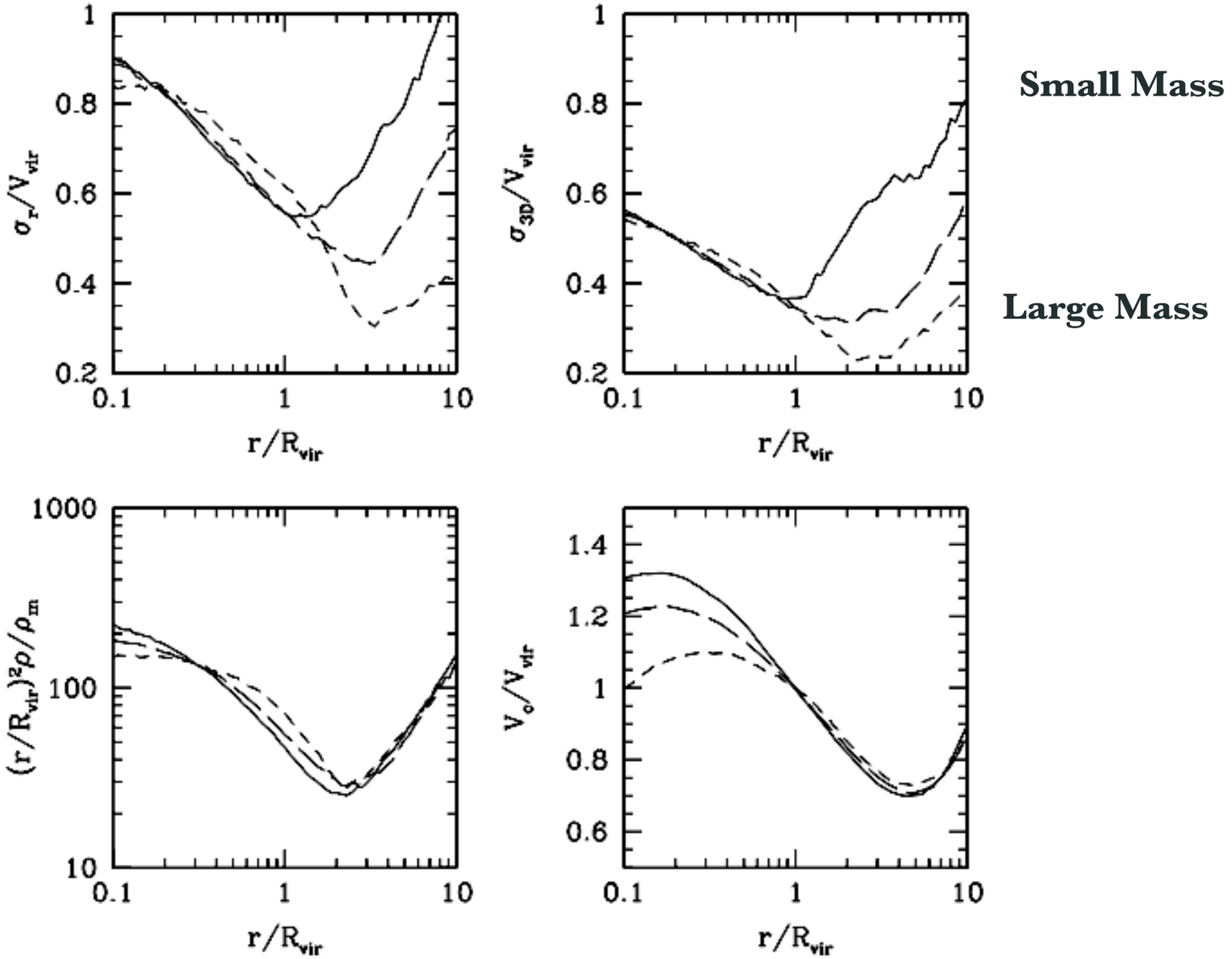

Figure 5. Median profiles for the same halo mass bins as in Figure 4. These profiles show how the behaviour of haloes depends on the halo mass. Top left panel: radial velocity dispersion. Top right: 3D velocity dispersion. Bottom left: density profile. Bottom right: Circular velocity profile. The different line styles represent the same mass bins as in Figure 4.

Halo Concentrations

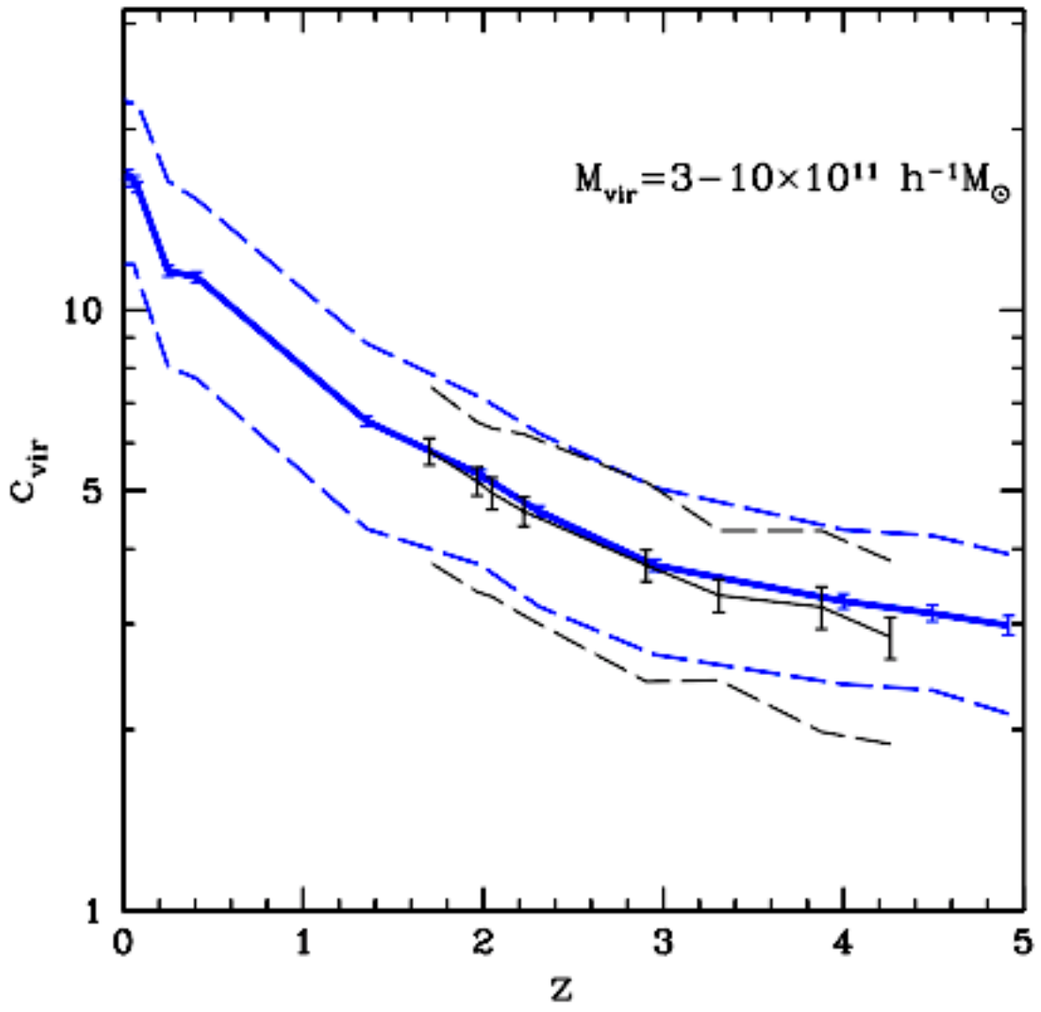

Figure 3. Convergence test for $c_{\rm vir}$ evolution and scatter. Shown is a comparison of $M_{\rm vir} = 3-10\times10^{11}h^{-1}M_\odot$ haloes simulated using our main simulation (thick lines) and a second simulation with 8 times the mass resolution (thin lines). The solid lines and errors reflect the median and Poisson uncertainty respectively. The dashed lines reflect the estimated intrinsic scatter. There is no evidence for significant deviations in either the measured median or scatter as the mass resolution is increased.

- Main trend with redshift

for a fixed halo mass

$$c_{\rm vir}(a) \propto a.$$

$$C \equiv \frac{r_{\rm vir}}{r_s},$$

$$r_{\rm vir}(M_{\rm vir}) = 443\ h^{-1}\ {\rm kpc}\left(\frac{M_{\rm vir}/10^{11}\ h^{-1}\ M_\odot}{\Omega_0\,\delta_{\rm th}}\right)^{1/3}$$

$$M_{\rm vir} \equiv \frac{4\pi}{3}\,\rho_{\rm cr}\,\Omega_0\,\delta_{\rm th}\,r_{\rm vir}^3\ .$$

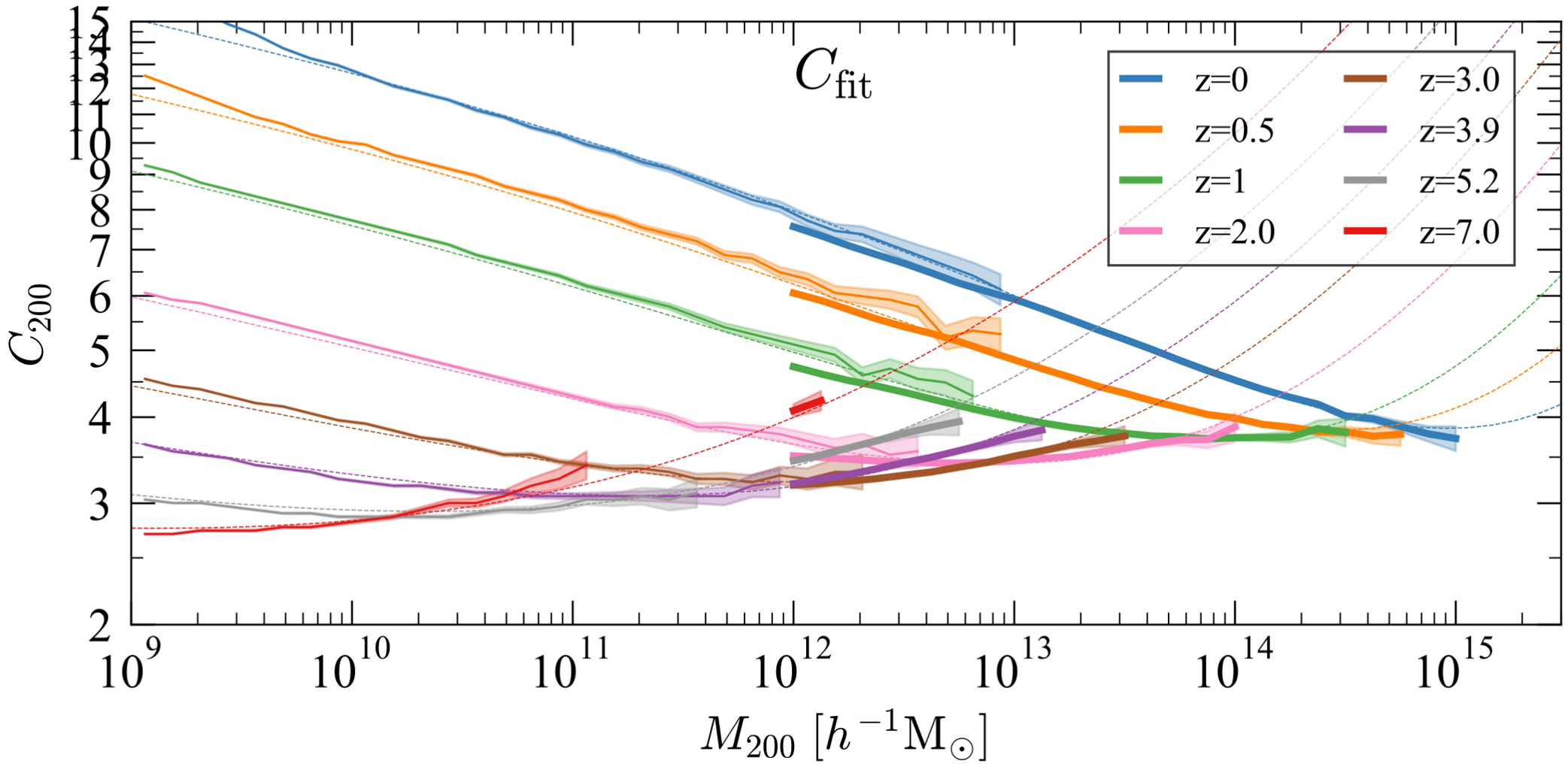
$C_{\rm fit}$
z=0
z=0.5
z=1
z=2.0
z=3.0
z=3.9
z=5.2
z=7.0
C_{200}
M_{200} $[h^{-1}{\rm M}_\odot]$

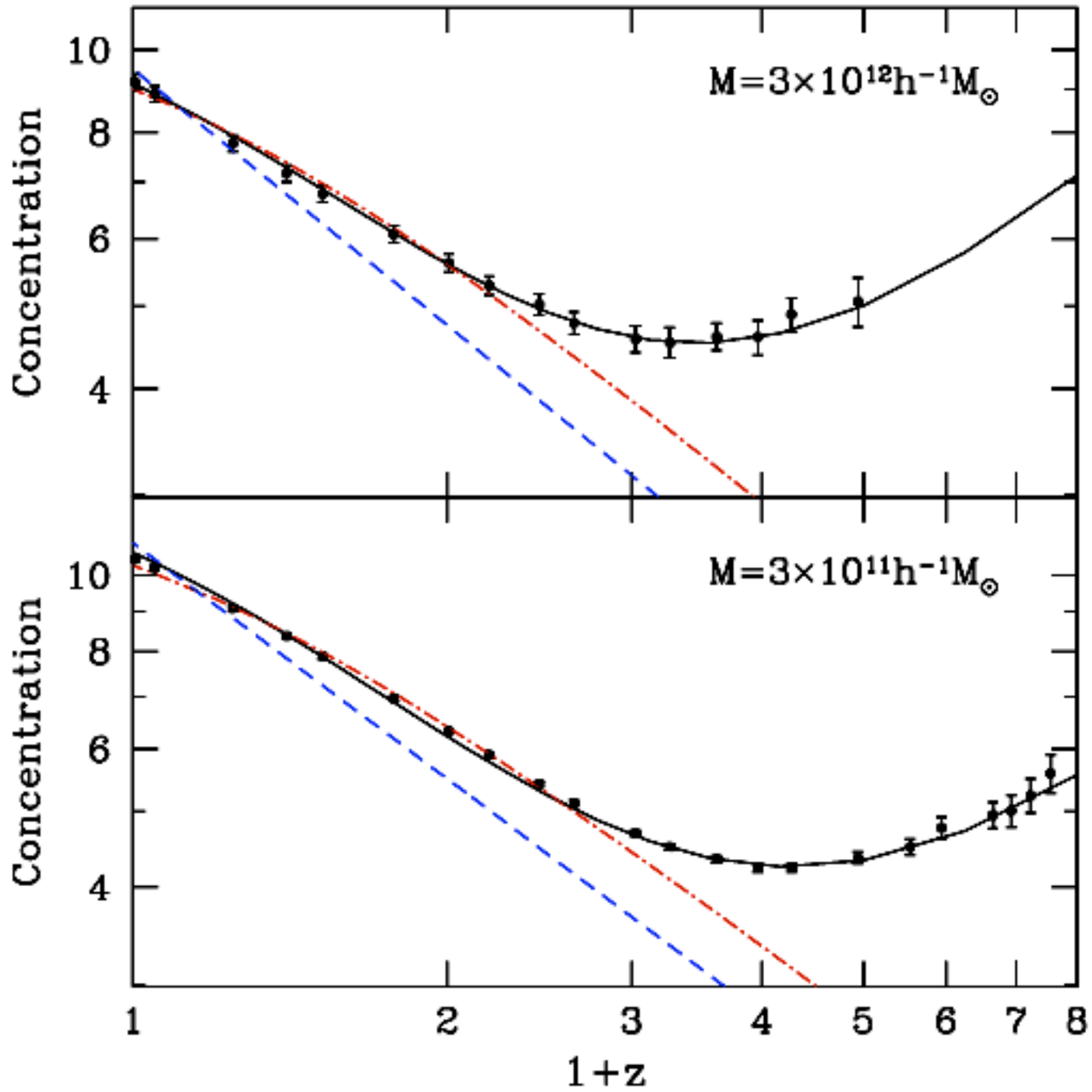

Figure 6. Evolution of halo concentration for halos with two masses indicated on the plot. The dots show results of simulations. For the reference the dashed lines show a power-law decline $c \propto (1+z)^{-1}$. Concentrations do not change as fast as the law predicts. At low redshifts $z < 2$ the decline in concentration is $c \propto \delta$ (dot-dashed curves), where δ is the linear growth factor. At high redshifts the concentration flattens and then slightly increases with mass. For both masses the concentration reaches a minimum of $c_{\rm min} \approx 4$–4.5, but the minimum happens at different redshifts for different masses. The full curves are analytical fits with the functional form of Equation (13).

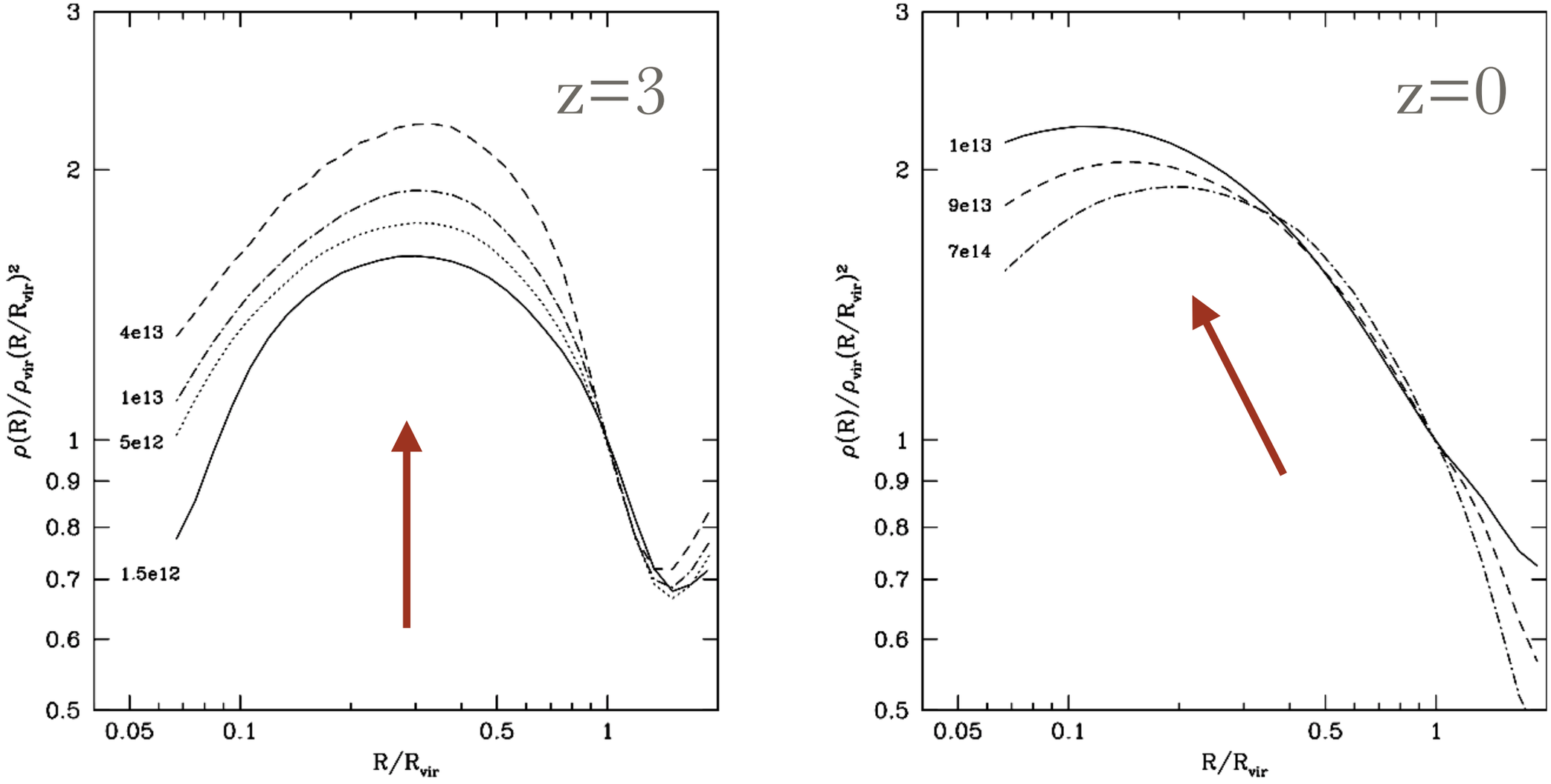

Median density profiles of relaxed halos at different redshifts and masses in N-body simulations. Profiles are normalized to have the same density at the virial radius. The left panel is for halos at z = 3: halos with larger mass are clearly more concentrated than halos with smaller masses. Similar to Einasto profiles in Figure 7, value of r_{-2} radius almost does not change with halo mass, which indicates that the increase in the concentration is mostly due to the increase in shape parameter α. The right panel shows profiles of halos at z = 0. Note that the trend with mass is different: more massive halos are less concentrated and r_{-2} radius decreases with decreasing mass.

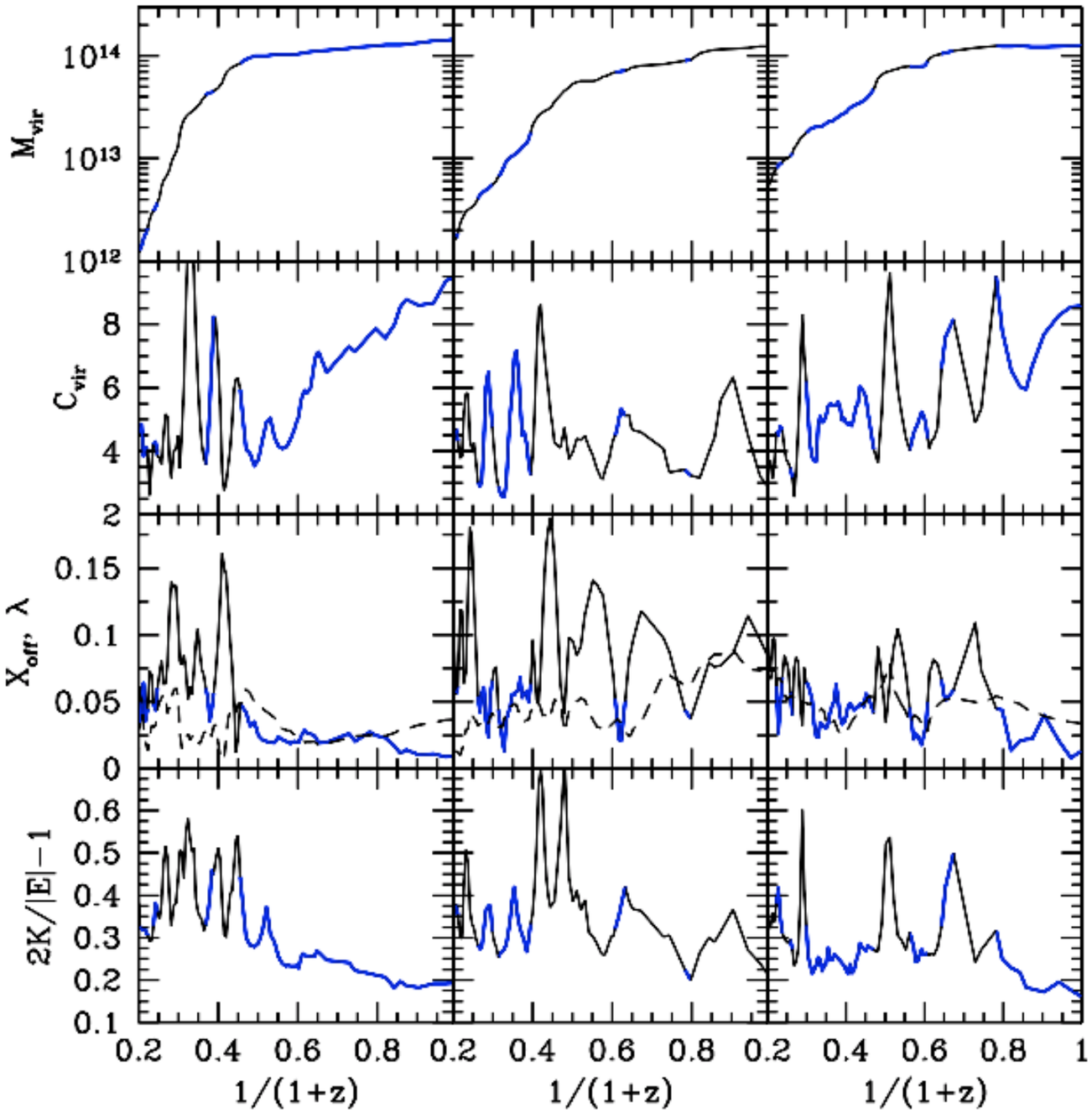

Examples of the evolution of virial mass M_{vir} , concentration C_{vir}, spin parameter λ (dashed curves in the second from the bottom panels), offset parameter X_{off} , and virial ratio 2K/|E| – 1 for 6 cluster-size halos taken from the BolshoiP simulation. Halos were selected to have $M_{vir} \approx 10^{14} h^{-1} M_{\odot}$ and be relaxed at z = 0. Thick solid (blue) parts of the curves indicate that halos are considered to be relaxed. Large variations in halo concentration are seen at high redshifts when the halo mass increases very quickly. Once the mass accretion slows down at low redshifts, halo concentration shows the tendency to increase. Major merger events, in the right panels, seen as large jumps in mass are followed by temporary increase in halo concentration. Most of these major-merger spikes in concentration are identified as happening in non-relaxed halos.

Density Profiles: Mass at ~1 kpc radius. Core-cusp problem

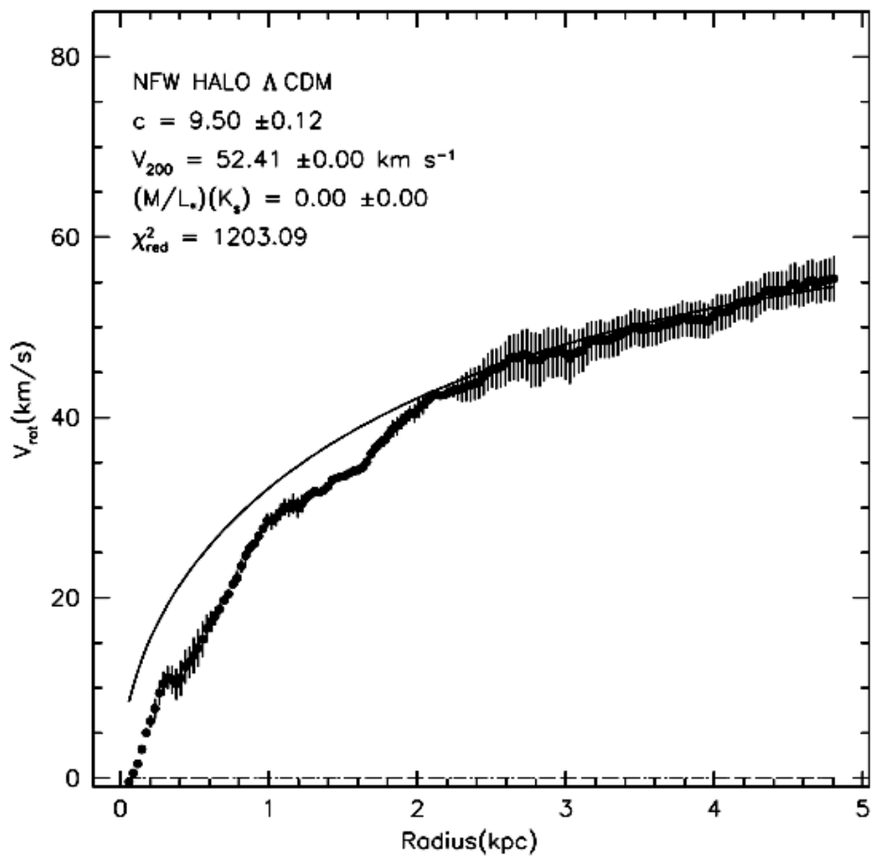

NGC 6822, de Blok etal 2007

Oh et al 2011

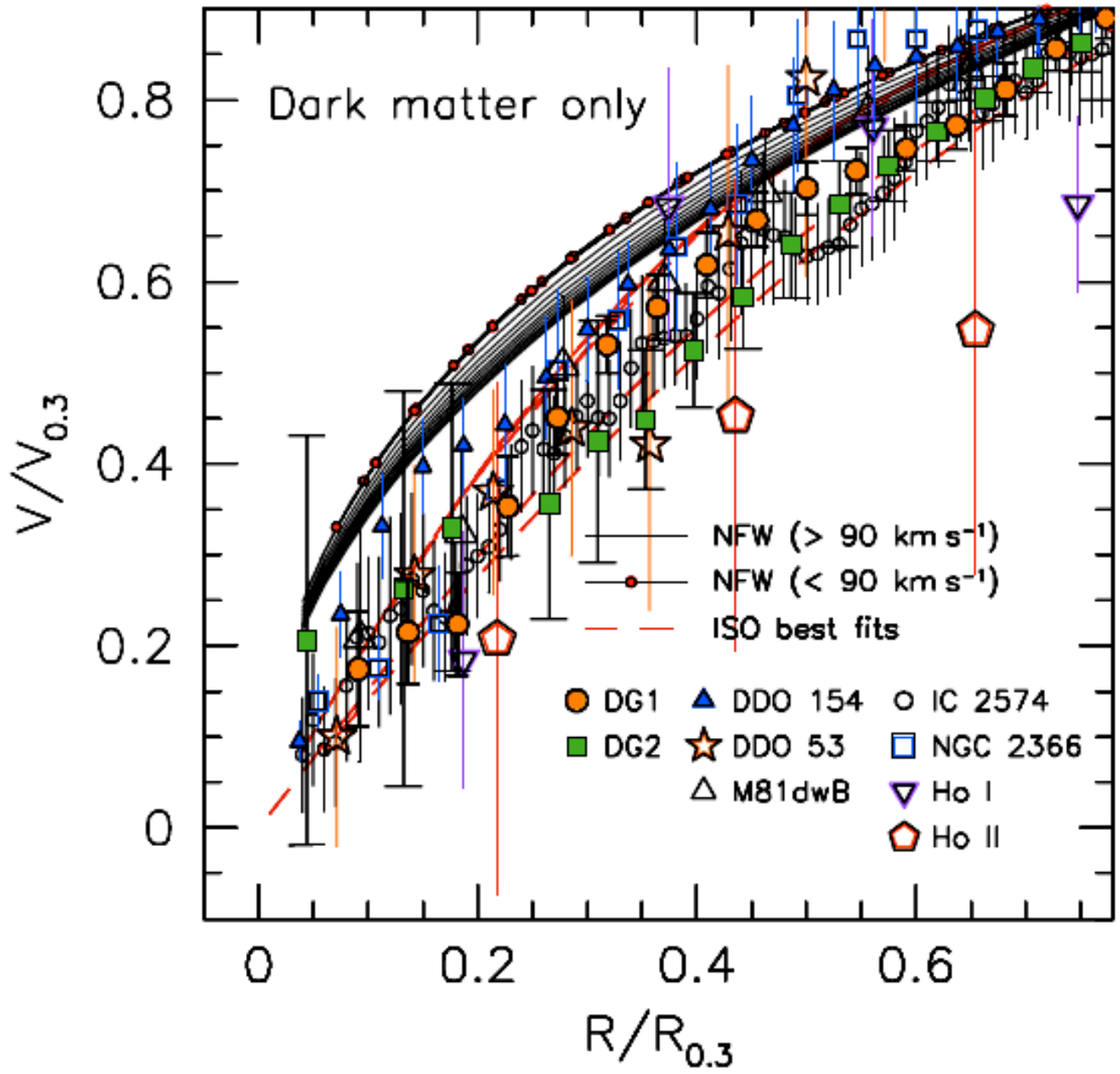

Numerous episodes of baryon infall followed by a strong burst of star formation, which expels the baryons. At the beginning of each episode the baryons dominate the gravitational potential. The DM contracts to respond to the changed potential. A sudden onset of star formation drives the baryons out. The DM also moves out because of the shallower potential. Each episode produces a relatively small effect on the DM, but a large number of them results in a significant decline of the DM density. Indeed, cosmological simulations that implement this process show a strong decline of the DM density. Whether the process happens in reality is still unclear.

Simulations with the cycles of infall-burst-expansion show flattening of the DM cusp may occur. If this happened to our Galaxy, then the DM density within the central ~ 500 pc may become constant. This would reduce the annihilation signal by orders of magnitude. We note that this mechanism would wipe out the DM cusp also in centers of dwarf galaxies.

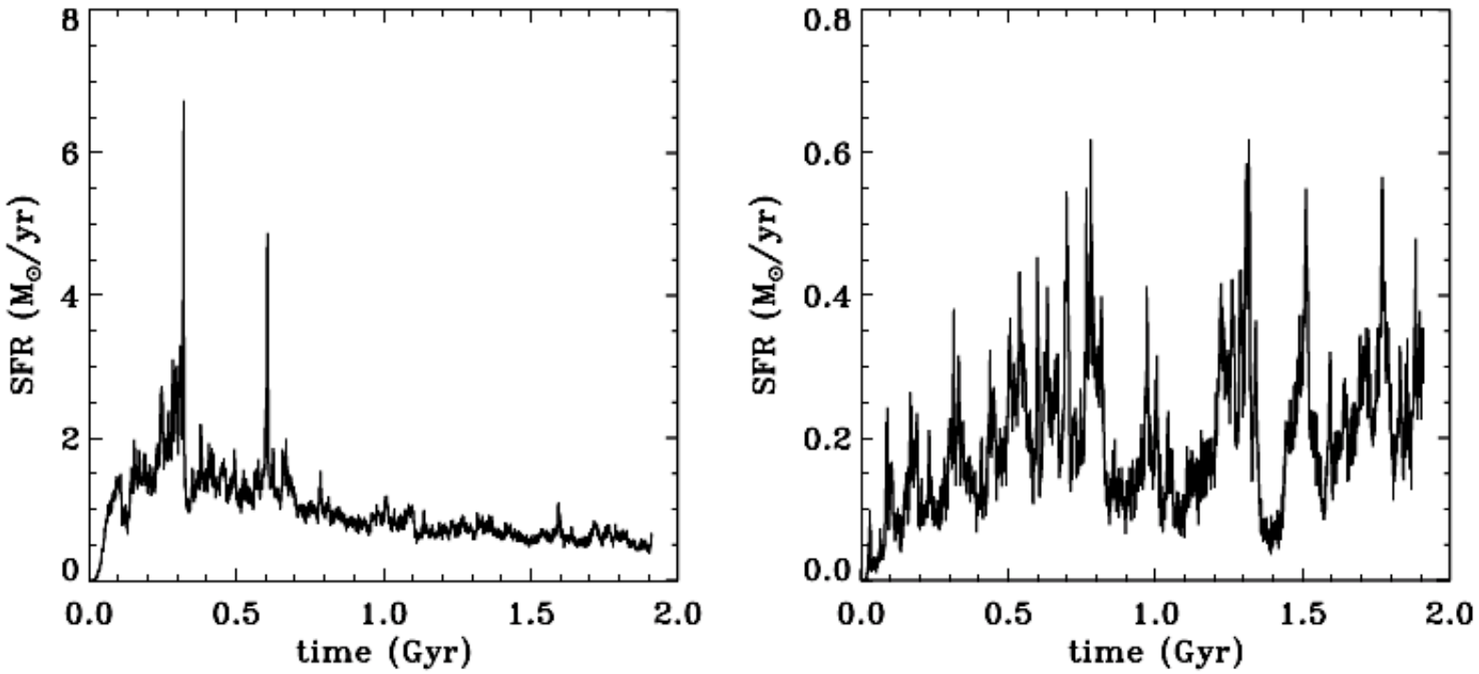

Figure 3. Star formation history in the runs without (left-hand plot) and with (right-hand plot) feedback.

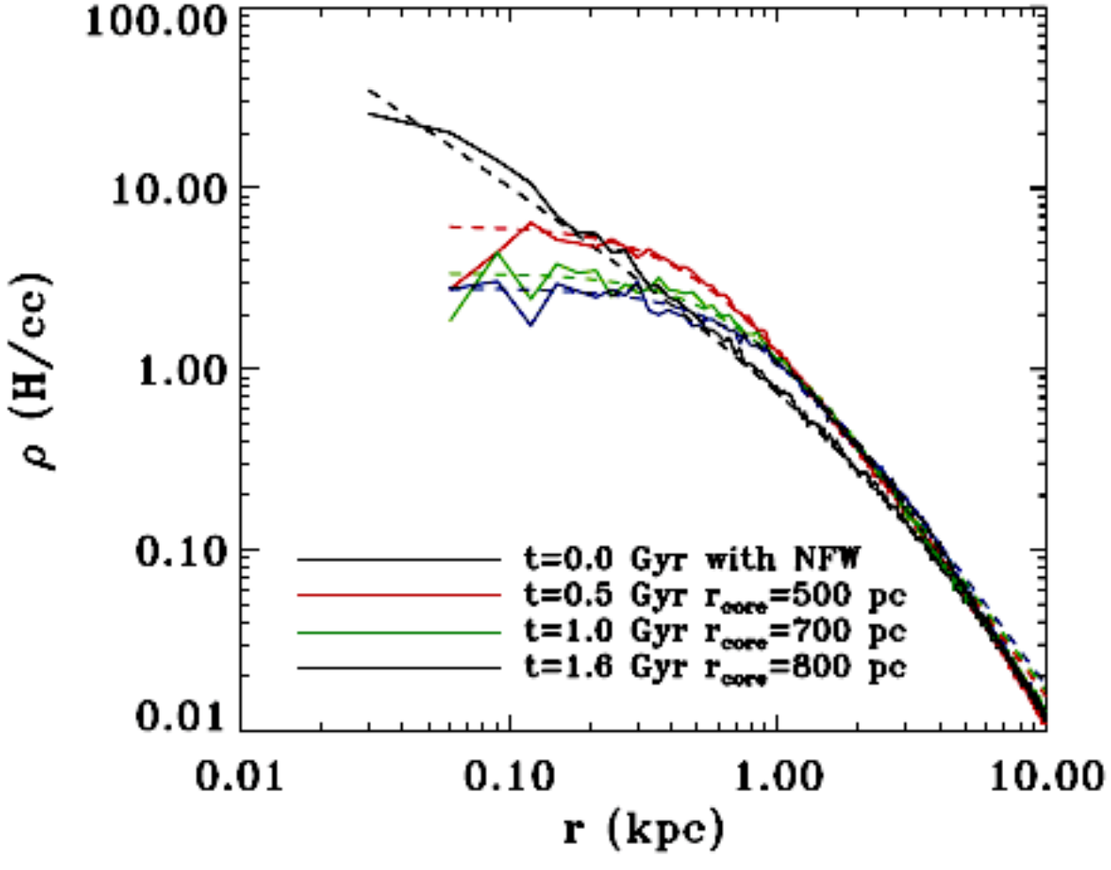

Figure 5. Evolution of the dark matter density profile over the 2Gyr of evolution for the control run with cooling, star formation and stellar feedback. We see the formation of a large core. We also show for comparison the analytical fit (dashed line) based on a pseudo-isothermal profile.

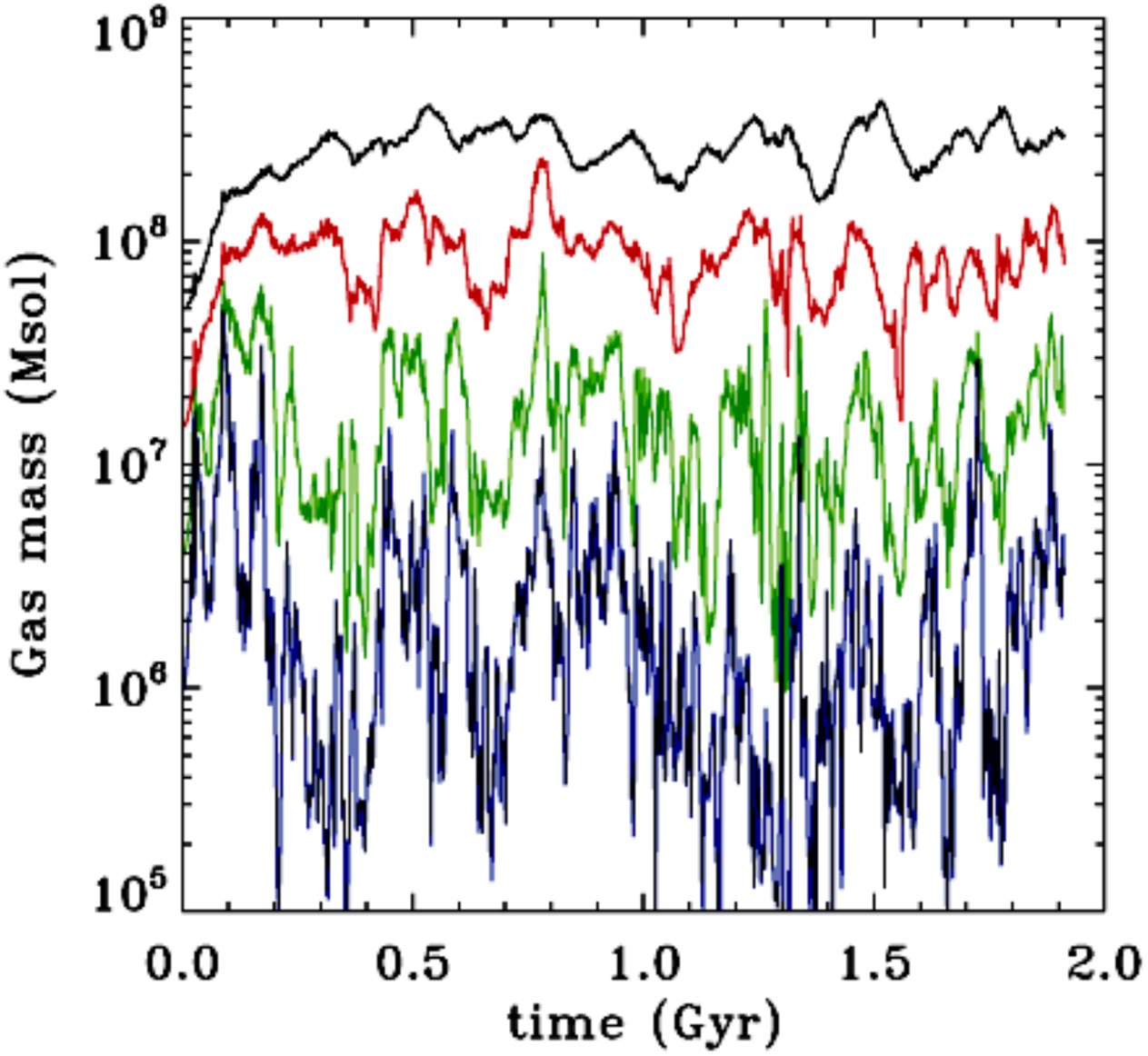

Figure 7. Time evolution of the total enclosed gas mass within spheres of radii 200 (blue), 400 (green), 800 (red) and 1600 (black) pc for the simulation with feedback.

Bridging the gap between halos and galaxies:

Milky Way: just an example of a dark matter distribution

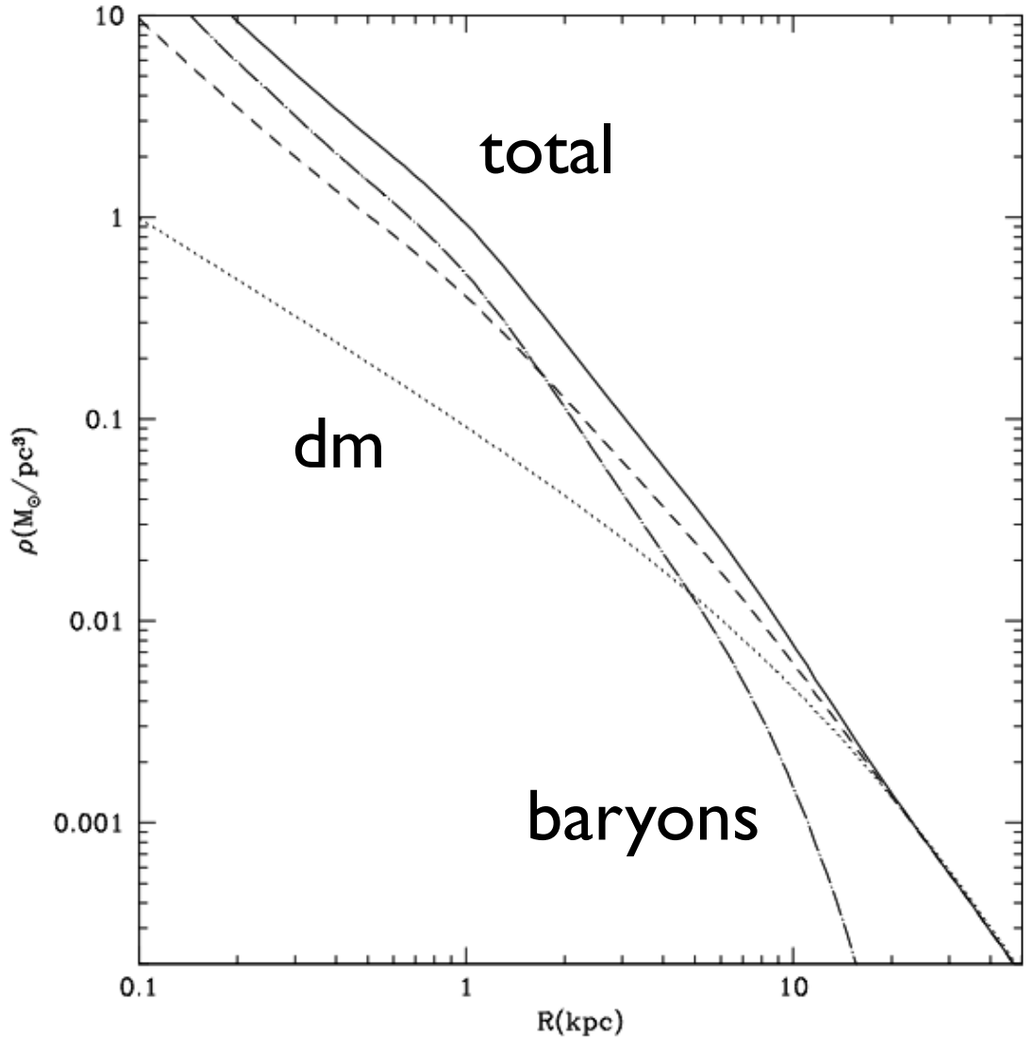

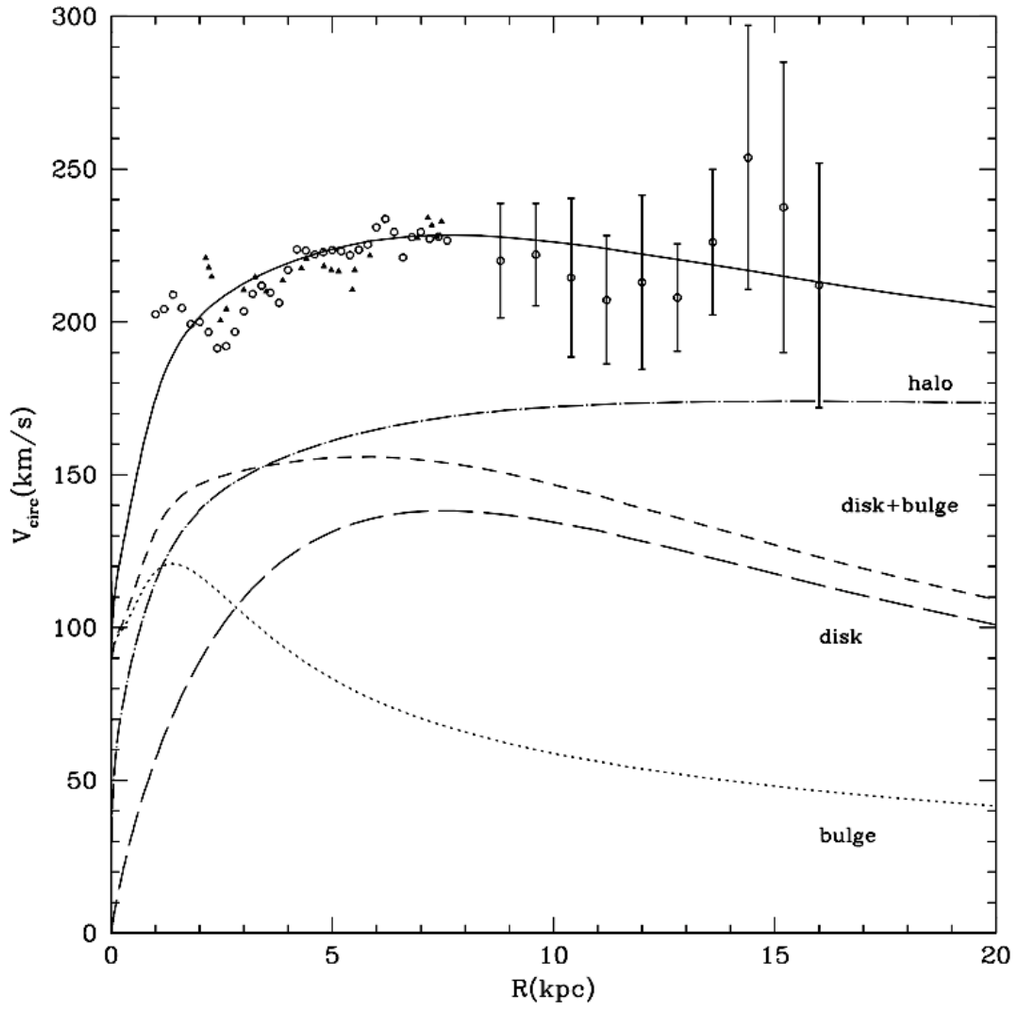

For each halo we find mass within given radius
M(<r) and then find maximum of circular velocity

$$V_{\rm circ} = \sqrt{\frac{GM(<r)}{r}}\Big|_{\rm max}$$

Fig. 5.— Effect of cold baryons on circular velocity profiles for three characteristic models of galaxies with virial masses 10^{13} $M_\odot$ (top), 1.7×10^{12} $M_\odot$ (middle), and 7×10^{10} $M_\odot$ (bottom). The "DM" curves include a cosmological fraction of baryons that trace the dark matter distribution. The cold baryon mass is added to the true dark matter mass in calculating the circular velocity ("DM+Baryons"). The effect of adiabatic compression of the dark matter is included in the models named "DM+Baryons+AC". After adding the cold baryons the circular velocities are rather flat in the inner $5 - 10$ kpc regions.

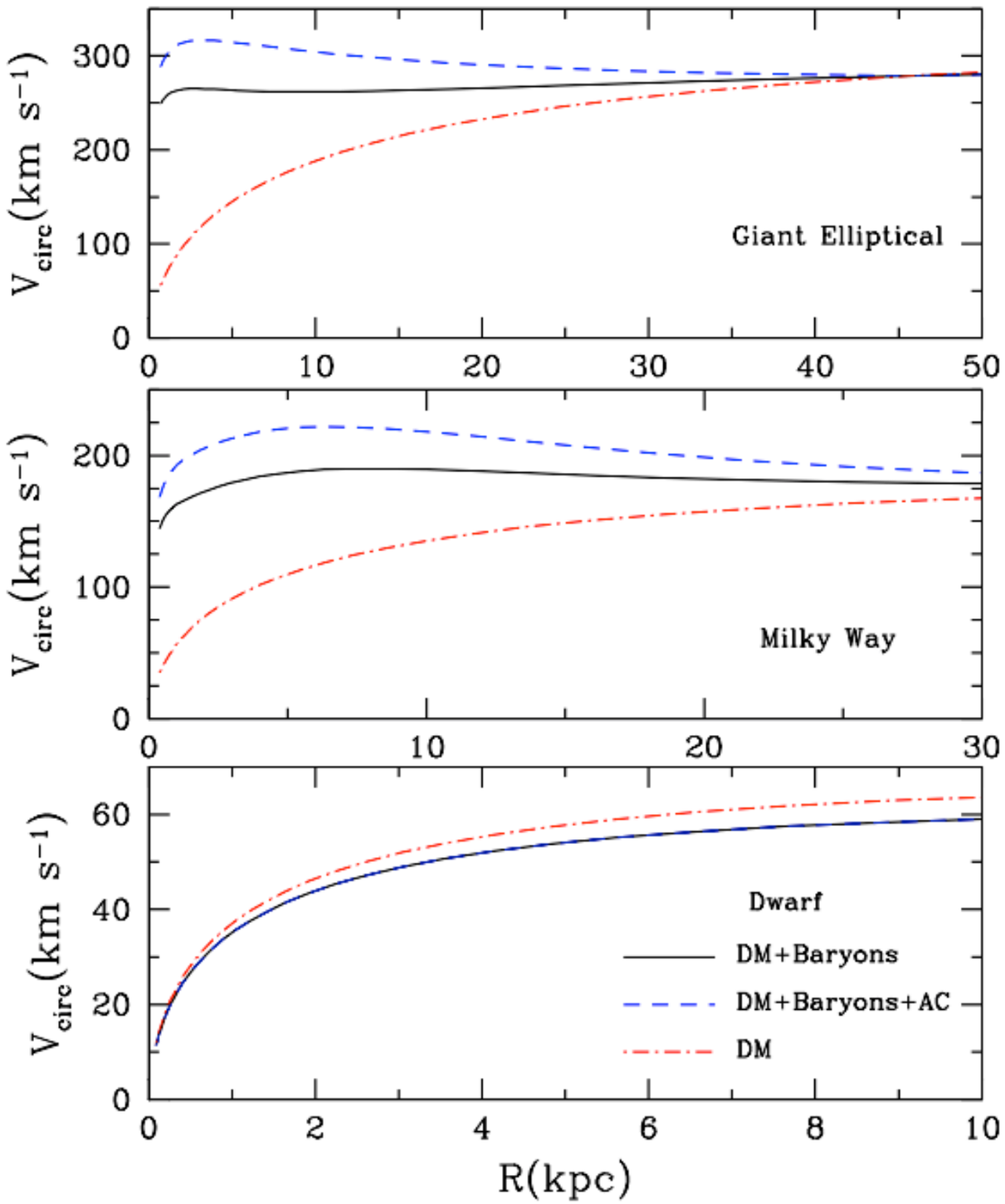

Internal dynamics of galaxies: TF and BTF

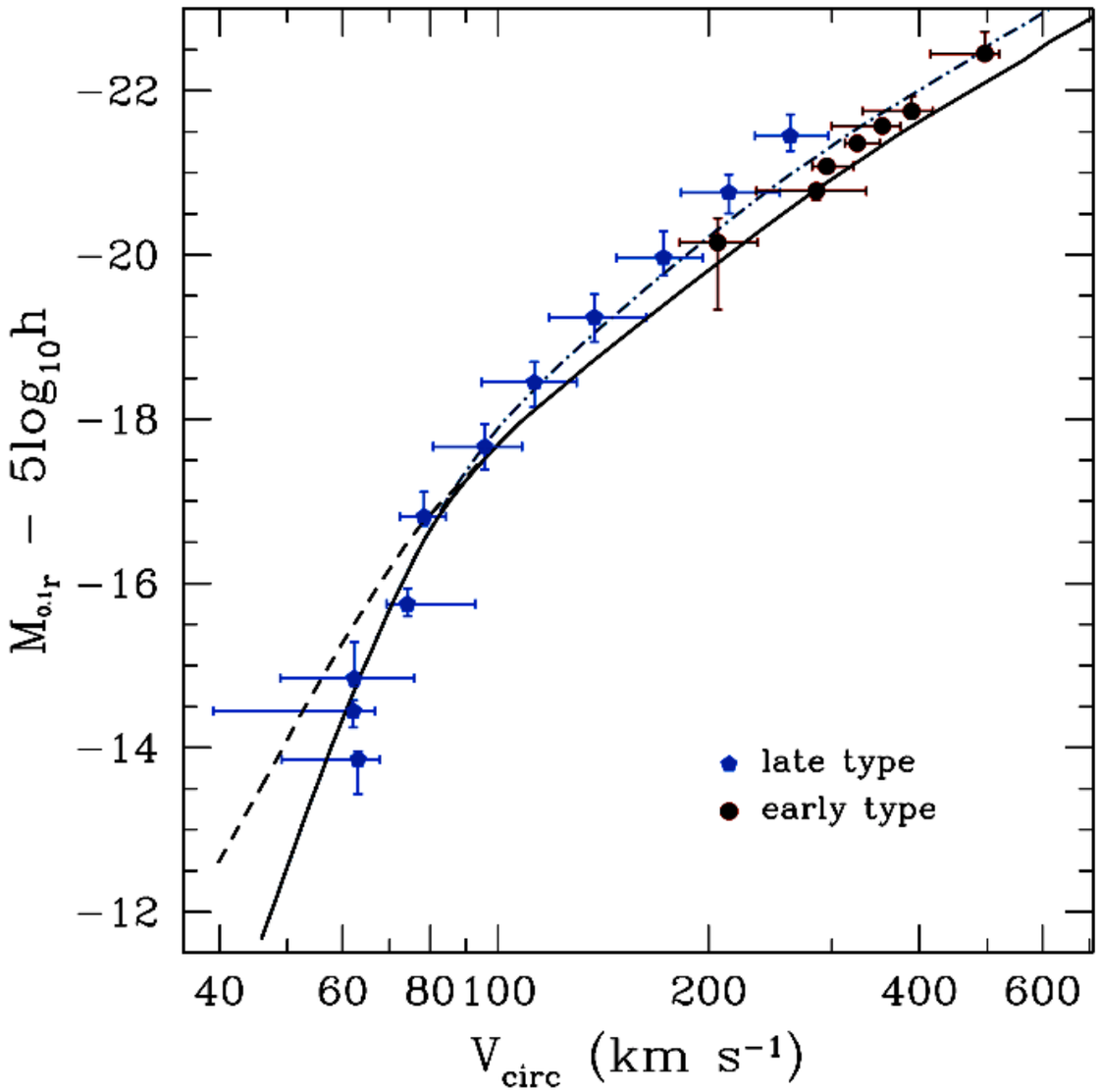

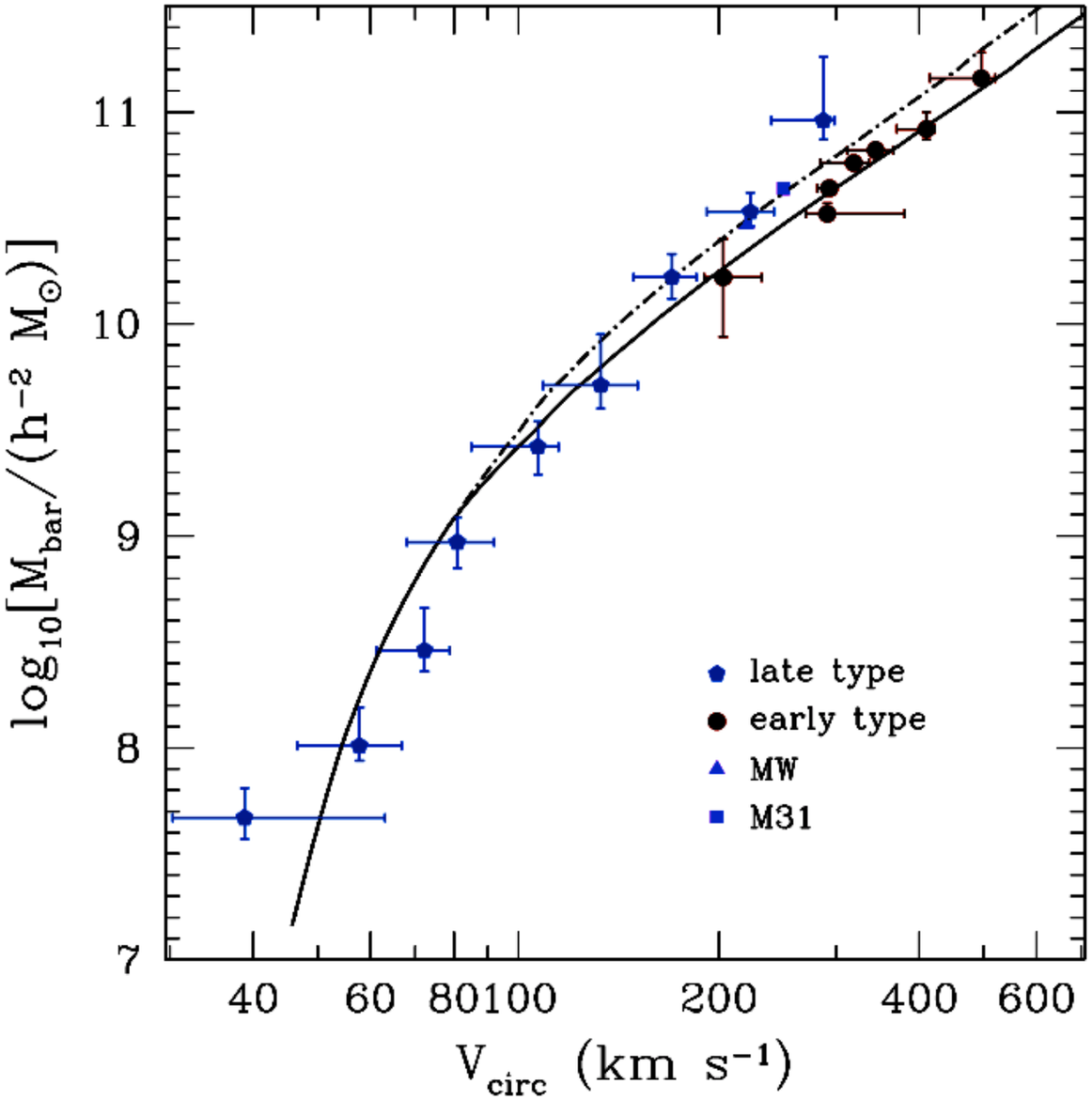

Halo Abundance matching: larger galaxies are hosted by bigger DM halos. No free parameters.

Trujillo-Gomez et al 2011

Lessons:

- Every galaxy is a dark matter halo
- No dark halos: if there is a dark matter concentration, it makes stars.

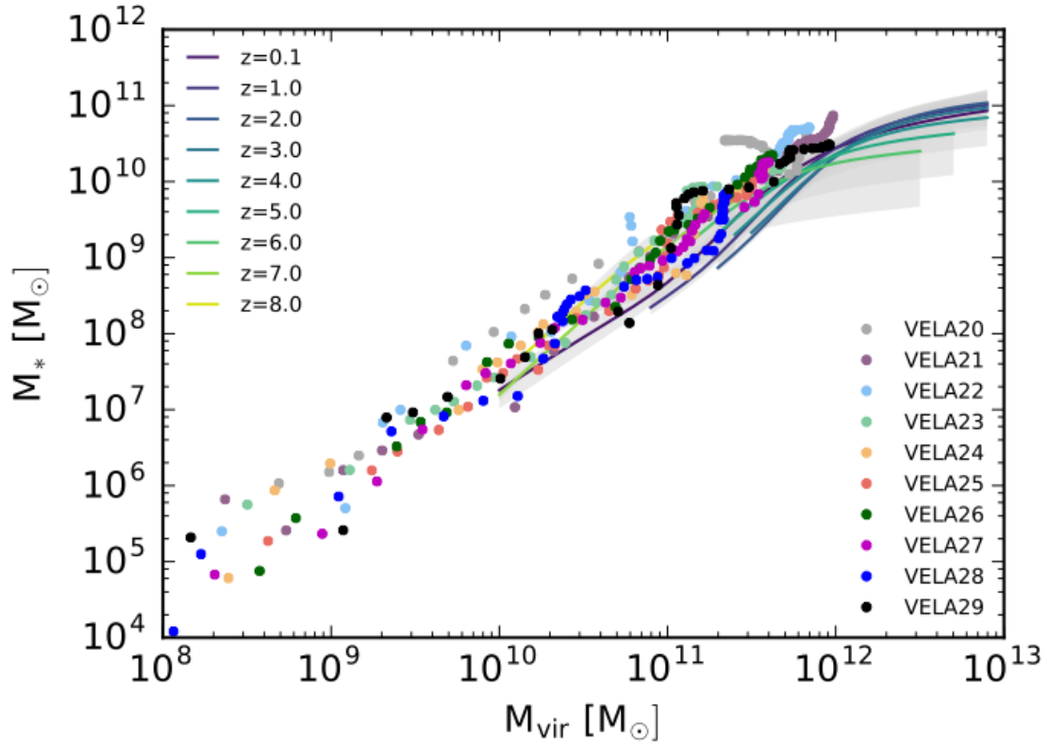

Bridging the gap between halos and galaxies:

Halo Occupation Distribution:

probability to find $N_{galaxies}$ in a distinct halo of mass M: $P(N_{galaxies}|M_{halo})$

- need to know how to get $P(N_{galaxies}|M_{halo})$
- need to know how to place 'galaxies'
- P(N|M) may depend on halo environment and dynamical state (e.g. merging ...)

Halo Abundance Matching (HAM):

- The biggest galaxy is hosted by the biggest halo and so on.
- There is some stochasticity between DM and stellar mass
- Subhalos must be resolved in simulations
- Needs merging trees of halos and subhalos

SDSS: z=0

DM galaxies

DM

SDSS

Correlation function

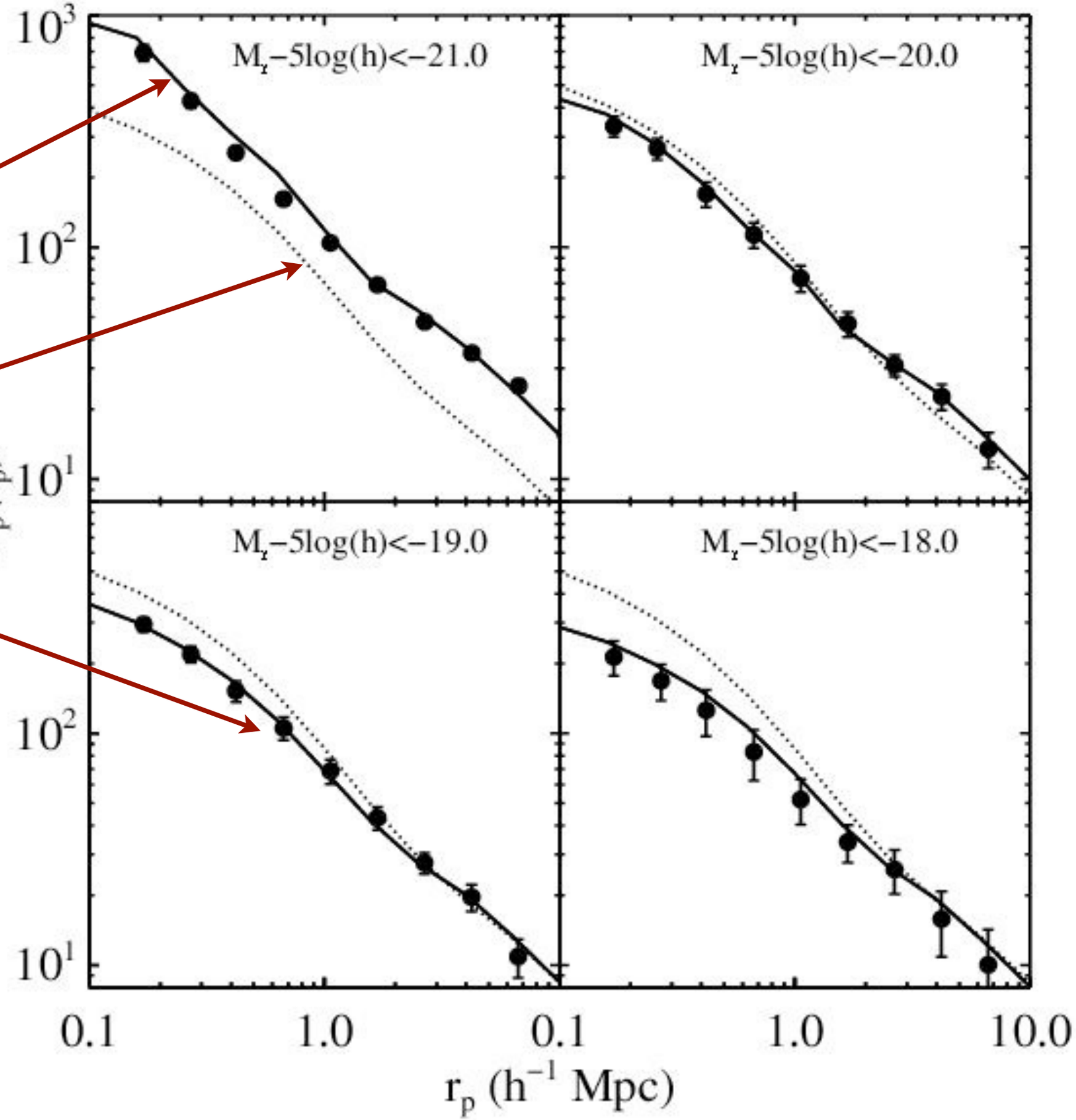

Halo Mass and Velocity functions

Functional form for mass function:

$$\frac{dn}{dM} = f(\sigma)\,\frac{\bar{\rho}_m}{M}\,\frac{d\ln\sigma^{-1}}{dM}$$

Average matter density:

$$\bar{\rho}_m(z) \equiv \Omega_m(z)\rho_{\rm crit}(z) = \bar{\rho}_m(0)(1+z)^3$$

Numerical factor:

$$f_{\rm P-S}(\sigma) = \sqrt{\frac{2}{\pi}}\,\frac{\delta_{\rm c}}{\sigma}\exp\left(-\frac{\delta_{\rm c}^2}{2\sigma^2}\right)$$

$$\delta_{\rm c} = 1.686$$

$$f_{\rm S-T}(\sigma) = A\sqrt{\frac{2a}{\pi}}\left[1+\left(\frac{\sigma^2}{a\delta_{\rm c}^2}\right)^p\right]\frac{\delta_{\rm c}}{\sigma}\exp\left(-\frac{a\delta_{\rm c}^2}{2\sigma^2}\right)$$

$$A = 0.3222,\ a = 0.707 \text{ and } p = 0.3$$

rms density fluctuation:

$$\sigma^2(M) = \frac{b^2(z)}{2\pi^2}\int_0^\infty k^2 P(k) W^2(k;M)\,{\rm d}k,$$

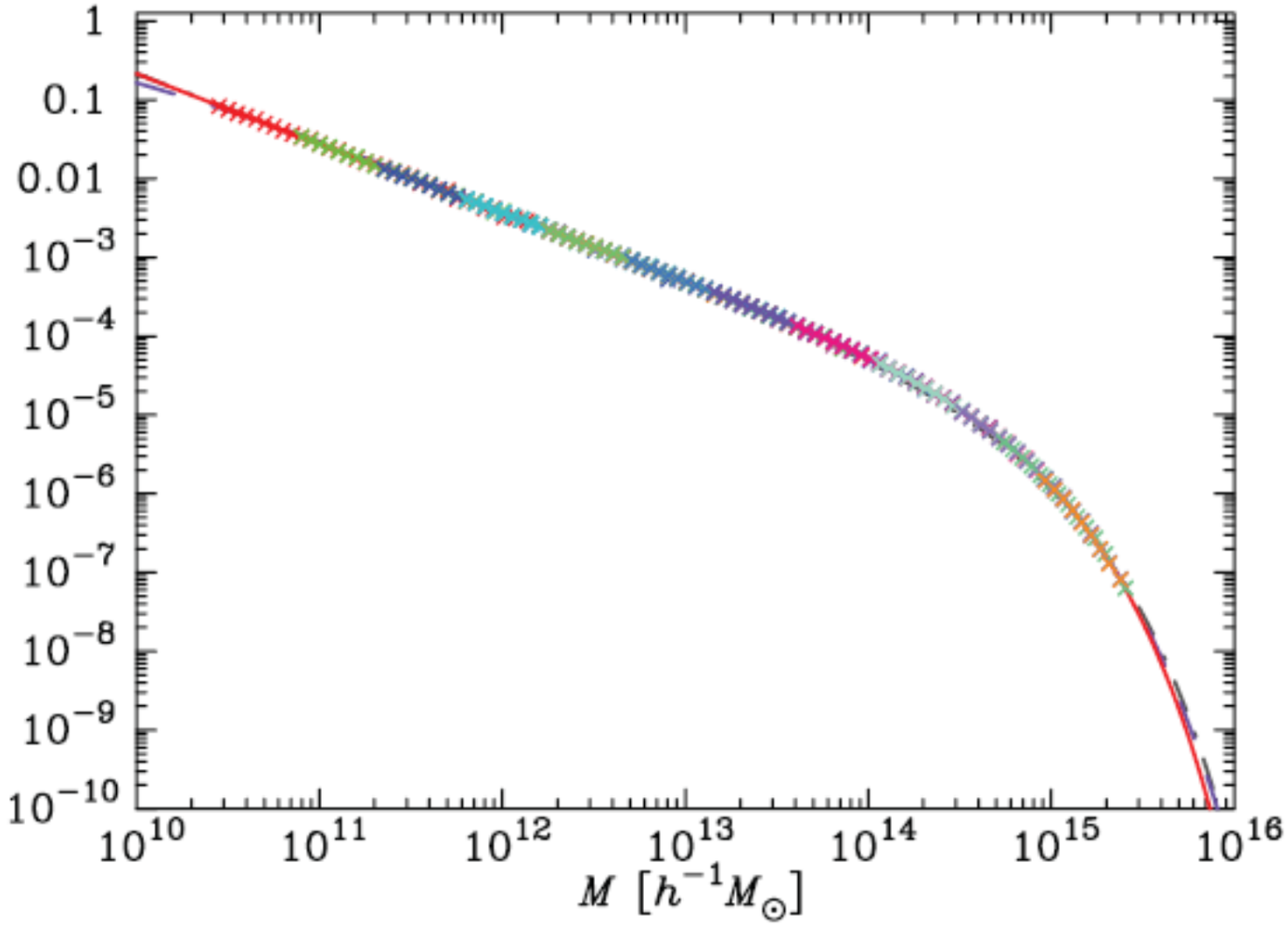

Warren et al 2006

FIG. 1.—Central values of the binned mass functions from sixteen 1024^3 simulations of the ΛCDM universe as crosses, with simulations in different colors. The best-fit form for the mass function we calculate is shown as a solid line (*red*), the Jenkins fit as a dashed line (*purple*), and the Sheth-Tormen fit as a dot-dashed line (*dark gray*). Goodness of fit is poorly judged on this extreme log scale; it is more clearly resolved in the linear residuals of Fig. 2.

Evolution of the mass function with redshift

Full curves are for the Sheth-Torman approximation

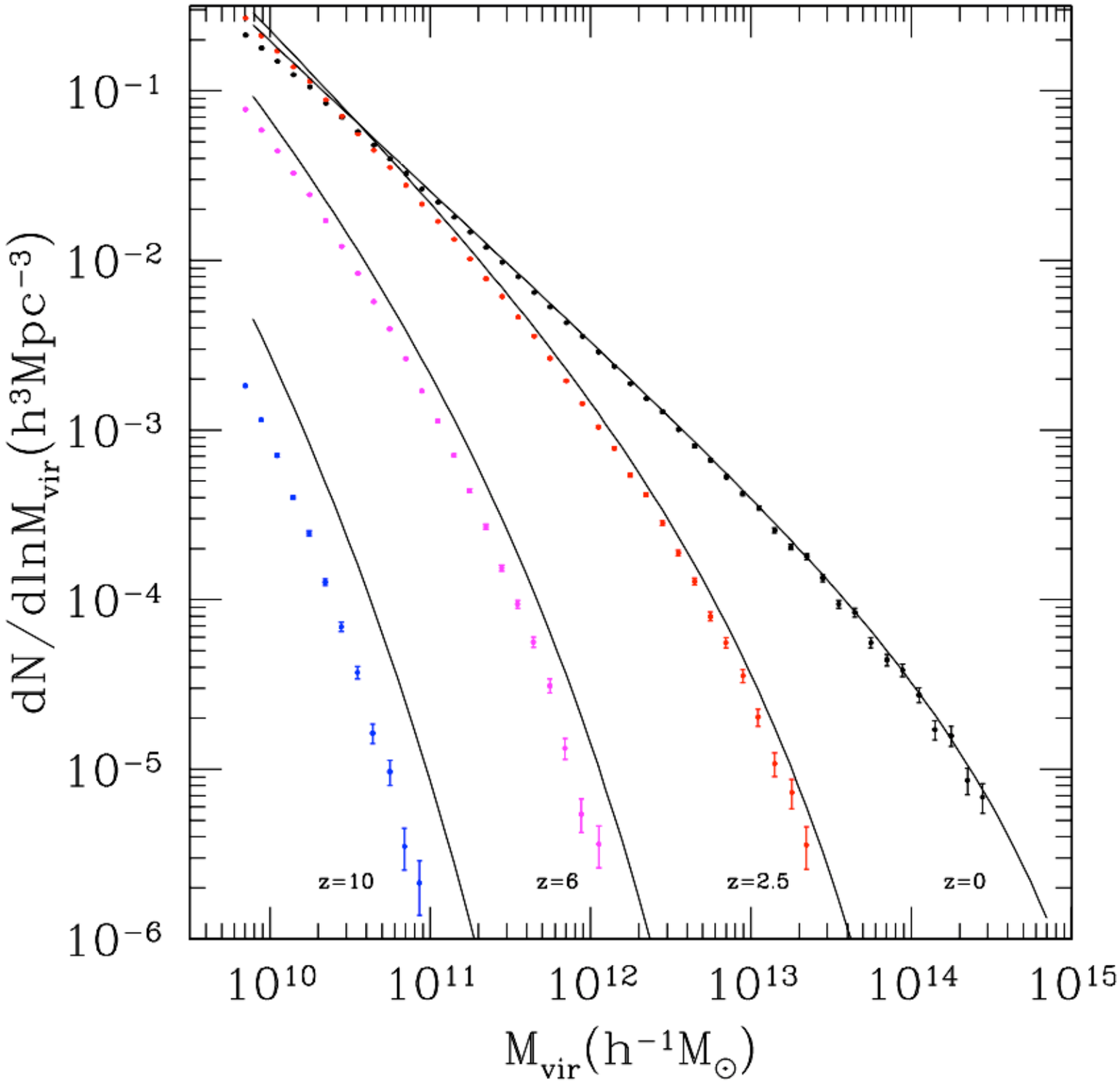

Symbols are from N-body simulations for distinct halos defined using Spherical Overdensity algorithm

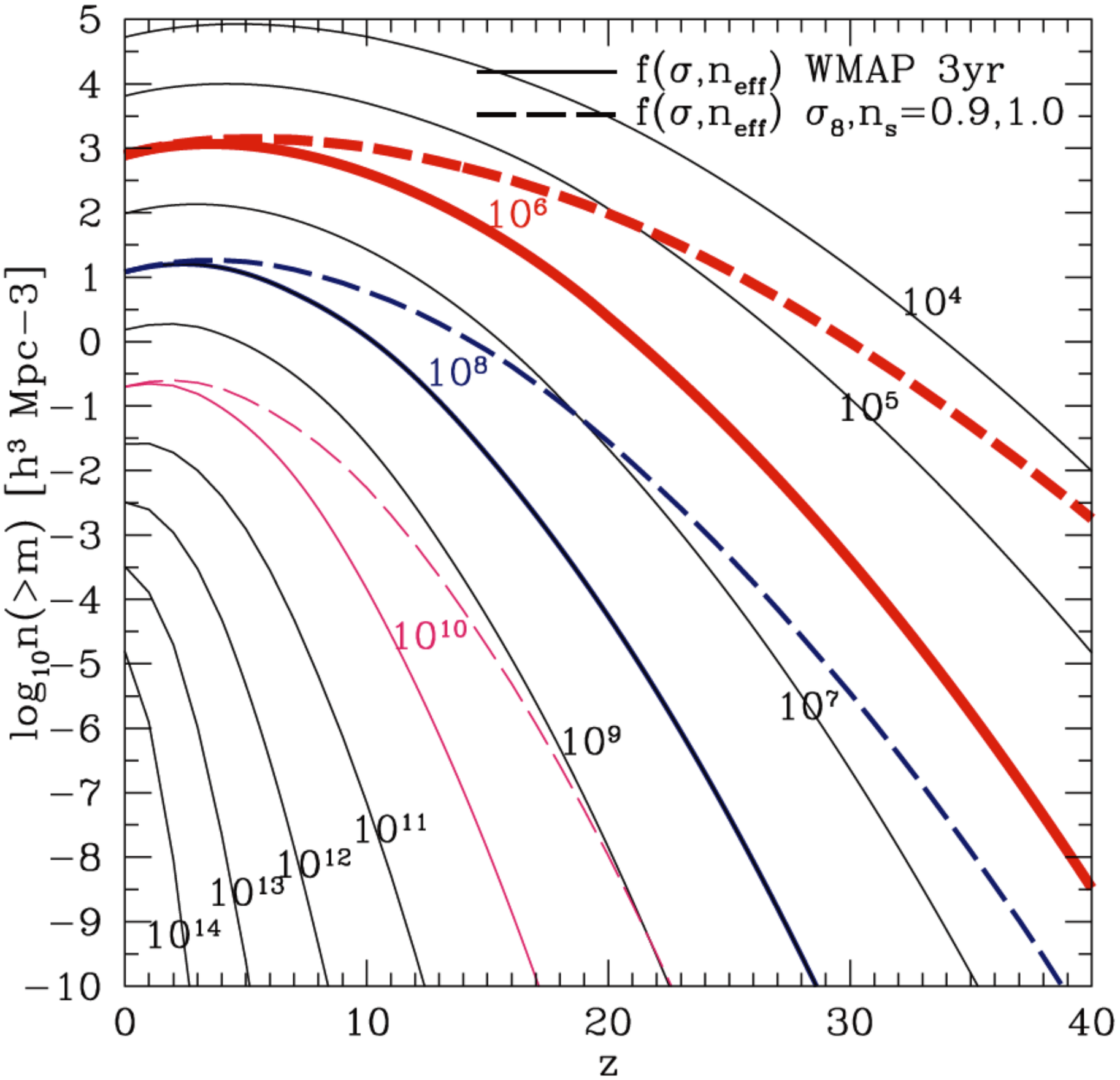
f(σ,n_eff) WMAP 3yr
f(σ,n_eff) σ_8,n_s=0.9,1.0
10^4
10^5
10^6
10^7
10^8
10^9
10^10
10^11
10^12
10^13
10^14
log_10 n(>m) [h^3 Mpc^-3]
z
5
4
3
2
1
0
−1
−2
−3
−4
−5
−6
−7
−8
−9
−10
0
10
20
30
40

Halo Velocity function

For each halo we find mass within given radius
M(<r) and then find maximum of circular velocity

$$V_{\rm circ} = \sqrt{\frac{GM(<r)}{r}}\Big|_{\rm max}$$

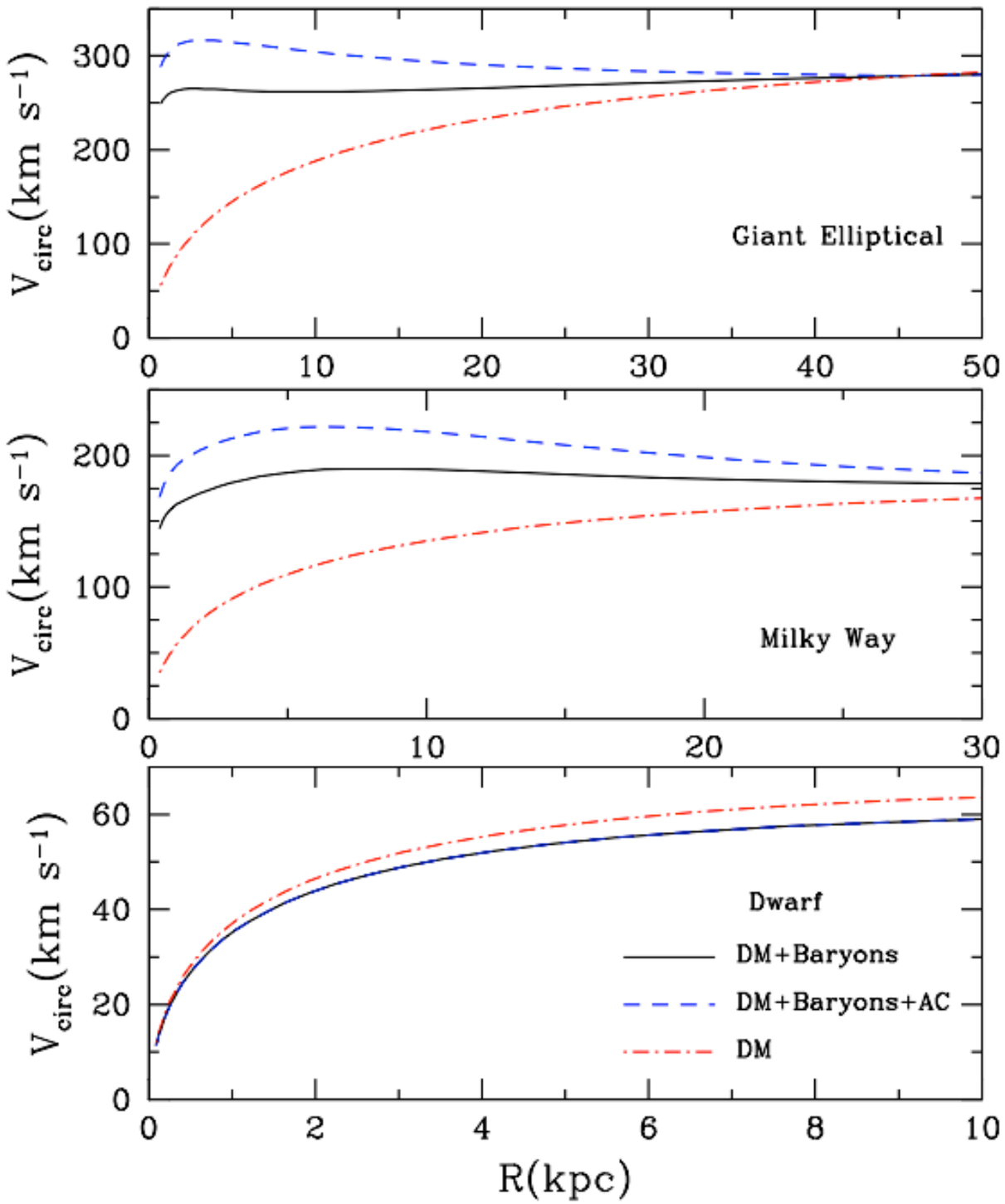

Fig. 5.— Effect of cold baryons on circular velocity profiles for three characteristic models of galaxies with virial masses 10^{13} $M_\odot$ (top), 1.7×10^{12} $M_\odot$ (middle), and 7×10^{10} $M_\odot$ (bottom). The "DM" curves include a cosmological fraction of baryons that trace the dark matter distribution. The cold baryon mass is added to the true dark matter mass in calculating the circular velocity ("DM+Baryons"). The effect of adiabatic compression of the dark matter is included in the models named "DM+Baryons+AC". After adding the cold baryons the circular velocities are rather flat in the inner $5 - 10$ kpc regions.

Halo Velocity function